
CONTROL OF THE POWER FLOWS OF A STOCHASTIC POWER SYSTEM

Zhen Wang ^{*}, Kaihua Xi[†], Aijie Cheng [†], Hai Xiang Lin [‡], Jan H. van Schuppen [‡]

July 16, 2024

ABSTRACT

How to determine the vector of power supplies of a stochastic power system for the next short horizon, such that the probability is less than a prespecified value that any phase-angle difference of a power line of the power network exits from a safe set? The power system is modelled such that the differential equation of each frequency is affected by a Brownian motion process. A safe set can be selected to be any subset of the interval $(-2 > + 2)$, which is a sufficient condition for not losing synchronization. That the controlled system has an improved performance is shown by numerical results of three academic examples including a particular eight-node academic network, a twelve-node ring network, and a Manhattan-grid network.

Keywords and Phrases: power systems, control of the power flows, optimization of the power supply vector.

1 Introduction

The aim of this paper is to present the solution of a control problem for a power system which is subject to stochastic disturbances and which may be in danger of losing transient stability.

Motivation The motivation of this paper is the fact that current power systems experience fluctuations in power lines and that such fluctuations are expected to increase in intensity in the coming decades. The fluctuations of the power flows are due to the power sources, in particular to the renewable power sources including wind turbines, wind parks, solar panels, photovoltaic panels, biomass generators, tidal energy, all without online C_2 production. The power supplied by wind turbines and photovoltaic panels will not be steady during either short or long time scales, but will fluctuate with the weather and other factors. The fluctuations of power demand are expected to increase in intensity due to an increasing variety of power loads. The fluctuations of power flows in the power network endanger the transient stability of the power system, for which a form of control is needed, [18, 23].

Problem Introduction The overall control objective of this paper is to maintain transient stability of a stochastic power system.

Control is the focus of this paper. The control objective of transient stability of the stochastic power system is strengthened to include the additional control objective that the probability is less than a prespecified value that any of the

^{*}Zhen Wang is grateful to the Chinese Scholarship Council for financial support (grant number 202106220104) for his stay at Delft University of Technology in Delft, The Netherlands. Zhen Wang is with the School of Mathematics, Shandong University, Jinan, 250100, Shandong Province, China and visited the Dept. of Applied Mathematics, Delft University of Technology, Delft, The Netherlands from November 2021 to February 2024 (email: wangzhen17@mail.sdu.edu.cn, wangzhen17.sdu@vip.163.com).

[†]Kaihua Xi and Aijie Cheng are with the School of Mathematics, Shandong University, Jinan, 250100, Shandong Province, China (email: kxi@sdu.edu.cn, aijie@sdu.edu.cn).

[‡]Hai Xiang Lin and Jan H. van Schuppen are with the Dept. of Applied Mathematics, Delft University of Technology, Delft, The Netherlands (email: H.X.Lin@tudelft.nl, J.H.vanSchuppen@tudelft.nl).

phase-angle differences of a power line exits from the safe set $(-2 > +2)$ or from a strict subset of that set. The restriction to a safe set of the phase-angle differences rather than to a domain of attraction of the state set, is an important step, which was used in [57, 58]. The time index set is discretized into a sequence of short horizons of approximately 3 to 15 minutes.

Problem Determine a power supply vector such that the controlled power system has a probability less than a prescribed value that the phase-angle difference over any power line exits from the interval $(-2 > +2)$. Instead of the described set, an engineer may select a strictly smaller subset of $(-2 > +2)$. The vector of power supplies has to be based on a prediction of the power demand vector over the next future short horizon, so that equality of the sum of power supplies and the sum of power demands is obtained. The computed control input will be the power supply vector which is held constant for a period equal to the length of the short horizon.

Literature Review Since the voltage is assumed to be constant in the short horizon, we first refer to [41] for the computation of the first exit-time to voltage instability of the power system with uncertainties in future loading, which reference would be useful for the voltage stability problem. Our paper investigates the control of power flows by using a sequential optimization approach on power dispatch in a secondary or tertiary control framework that may be extended to the Security-Constrained Optimal Power Flow (SC-OPF) methodology in the future. An SC-OPF problem involves determining power dispatch while considering constraints such as generator capabilities and voltage limits, with optimization criteria including generator costs and transmission losses. Here, we first review the literature related to the SC-OPF so as to better address the literature of our problem. A comprehensive survey about the Security-Constrained Optimal Power Flow can be found in [5].

Security-Constrained Optimal Power Flow (SC-OPF) with constraints. [40], N. Ngaa et al. put the frequency deviation as a nonlinear constraint in the optimal power flow network and then used the genetic algorithm to solve the problem. They clarify the importance of considering this constraint. However, the dispatch cost will be higher than before caused by a preference for choosing a generator with higher inertia. Note that this paper considers both active power and reactive power. In [17], a differentiable function on power system variables is considered, which is extracted from the Neural network representation of the secure boundary. This approach can better approximate the secure boundary than a typical method, which uses as a constraint the OPF model for optimal dispatch.

[1, 2] consider transient stability as a constraint for power dispatch. [1] presents several techniques for the Transient Stability Constrained-Optimal Power Flow (TSC-OPF) problems. [2] proposed a directional derivative-based method to make the angle deviation from the center of inertia decrease in the steepest direction to determine a transiently-stable power dispatch, by this method only two constraints are added to the conventional optimal power flow framework. Two numerical experiments show that the increased cost of the proposed procedure from the conventional OPF analysis is quite minor.

The economic issue is addressed in the following references. [48] discuss using power router (PR) control in the security-constrained optimal power flow as a real-time power dispatch setpoint, where the PR phase-angle injection is included in the objective function and constraints. The economic cost is minimized while the constraints are still satisfied. In this literature, the AC power flow equation is used. Furthermore, the proposed algorithm is easy to be extended by the conventional SC-OPF algorithms. [37] considers system corrective capabilities into an economic dispatch problem with security constraints. By a decomposition technique which allows separate contingency analysis with generator rescheduling and an iterative procedure, the same security level of the conventional security-constrained dispatch can be achieved, while the economic cost is lower. Note that this work deals with AC power flows, not with linearized power flow. Load forecast and network configuration can be taken into account in their proposed framework, while these two items are strengthened in our paper.

A probabilistic framework is investigated in the following references. [51] extend the SC-OPF when incorporating renewable energy sources to a probabilistic robust one. They use simulation results to justify their choice by comparing the OPF, the SC-OPF, and the probabilistic robust SC-OPF. Furthermore, the performances of adopting AC and DC power flow are also compared, while the AC power flow model respects the violation level and the DC power flow does not. Moreover, the cost of the proposed corrective scheme (policy based Automatic Voltage Regulation (AVR) set-point) is lower than the constant AVR set-point. Furthermore, in this paper, a convex relaxation is used.

From a centralized manner to a distributed manner. [36] put forward two multi-agent distributed approaches to solve the DC Security Constraint Optimal Power Flow problem due to the urgent need for distributing integrated renewable sources like solar panels in a decentralized manner.

However, few papers have investigated analytically the stochastic fluctuations of power systems and their control. Even fewer papers presented concrete procedures to suppress or to mitigate the fluctuations of a power system with integrated renewable sources. In our paper, an AC power flow model is adopted.

Secondly, we review literature related to the H_2 norm. This is done because we investigate the stochastic power system in the manner of the invariant distribution of the stochastic linearized power system. [33] introduced a management with power supply and demand, and how the future power system would be like, from which one learns that renewable sources will replace the traditional generation gradually in the future and therefore the inertia will dramatically drop down to zero after the penetration of these renewable sources, [42] put forward an algorithm on where to place virtual inertia aiming to optimize a H_2 norm which is a global metric containing both phase-angle difference and frequency deviation. [47], H_2 norm is also used to evaluate the resistive power losses in terms of the design of future power systems where more generators and transmission lines should be accommodated. Note that in [42, 47], a linear DC model is used.

However, as already pointed out in [53] and later in Section 2.10, the variance of the power flow at one line or of a particular node can also be calculated by the H_2 norm of the input-output LTI system, setting the output as only the phase-angle difference at one line or as only the frequency at one node. If one wants to control the most vulnerable line or the most vulnerable node, one needs to solve many Lyapunov equations. Thus, the H_2 norm is not used in this paper.

Contributions of this Paper (1) A detailed derivation of the probability and of an upper bound on that probability that the phase-angle difference across any power line exits from a safe set according to an invariant probability distribution. (2) The numerical results for the optimal power supply vectors and of the phase-angle differences of the power line flows for three academic examples, including a particular eight-node example, a twelve-node ring network, and a small Manhattan-grid example. These three examples are chosen so as to investigate the influence of different network structures on the probabilities.

Paper Organization Section 2 introduces a deterministic power system and a stochastic linearized power system. The control objective function is introduced and defined in Section 3. The performance of the controlled power systems for three illustrative examples, based on their numerical computations, are summarized and displayed in Section 4. Section 5 states conclusions and describes open research issues. The reader may find results on a related optimization problem in the companion paper [55].

2 The Power System

2.1 Notation

The set of the integers is denoted by \mathbb{Z} and that of the positive integers by $\mathbb{Z}_+ = \{1, 2, \dots\}$. The natural numbers are denoted by $\mathbb{N} = \{0, 1, 2, \dots\}$. For any positive integer $k \in \mathbb{Z}_+$ denote the finite sets $\mathbb{Z}_k = \{1, 2, \dots, k\}$ and $\mathbb{N}_k = \{0, 1, 2, \dots, k\}$. The real numbers, the positive real numbers, and the strictly positive real numbers are respectively denoted by \mathbb{R} , $\mathbb{R}_+ = [0, \infty)$, and $\mathbb{R}_{s+} = (0, \infty)$. The complex numbers are denoted by \mathbb{C} . The open left part of the complex plane is denoted by $\mathbb{C}_o^- = \{z \in \mathbb{C} \mid \text{Re}(z) < 0\}$. Denote the *sign* function as, $\text{sign}(x) = +1$ if $x > 0$, -1 if $x < 0$, 0 otherwise.

The vector space of $n \in \mathbb{Z}_+$ tuples of the real numbers is denoted by \mathbb{R}^n . Denote by $\mathbf{1}_k$ the k -th unit vector whose k -th component equals one while the other components equal zero. Denote by $\mathbf{1}_n \in \mathbb{R}^n$, the n -dimensional vector whose components are all equal to 1. The set of matrices of size $n \times m$ with entries in the real numbers, is denoted by $\mathbb{R}^{n \times m}$. The n -th column of matrix A is denoted by A_n , and the n -th row of matrix A is denoted by $A(n)$. The set of matrices of size $n \times n$ with elements in the real numbers whose off-diagonal elements are all zeros is denoted by $\mathbb{R}_{diag}^{n \times n}$. Denote a diagonal matrix, with on the diagonal the elements of the vector $v \in \mathbb{R}^n$, by $\text{diag}(v) \in \mathbb{R}^{n \times n}$. A matrix $\bullet \in \mathbb{R}^{n \times n}$ is called *symmetric and positive definite* if for all $v \in \mathbb{R}^n$, $v^T \bullet v \geq 0$ and denote the set by $\mathbb{R}_{pds}^{n \times n}$. Such a matrix is called *strictly positive definite* if, for all $v \in \mathbb{R}^n$ with $v \neq 0$, $v^T \bullet v < 0$ and denote the set of such matrices by $\mathbb{R}_{spds}^{n \times n}$.

The spectrum of the square matrix $A \in \mathbb{R}^{n \times n}$ is denoted by $\text{spec}(A)$, which set is defined as the set of eigenvalues of that matrix. Denote the *spectral index* of matrix $A \in \mathbb{R}^{n \times n}$ as the tuple $n_{si}(A) = \{n_-, n_0, n_+\}$ where $n_- \in \mathbb{N}$ is the number of eigenvalues with strictly negative real part, thus in $\mathbb{C}_o^- = \{z \in \mathbb{C} \mid \text{Re}(z) < 0\}$, $n_0 \in \mathbb{N}$ is the number of eigenvalues with real part equal to zero, and $n_+ \in \mathbb{N}$ is the number of eigenvalues with strictly positive real part, thus in $\mathbb{C}_o^+ = \{z \in \mathbb{C} \mid \text{Re}(z) > 0\}$.

The symbol $x \in G(x \succ x)$ denotes that the random variable $x : \Omega \rightarrow \mathbb{R}^n$ has a Gaussian probability distribution function with mean $\bar{x} \in \mathbb{R}^n$ and variance $\bullet_x \in \mathbb{R}_{pds}^{n \times n}$.

2.2 The Deterministic Nonlinear Power System

The *nonlinear power system* is defined by a set of nonlinear differential equations driven by the input signal p , [26], [20], [3], and [9]. The *nominal frequency* is defined to be the frequency of a rotating frame with respect to which the actual power system will be defined. The value of the nominal frequency equals 50 Hz in Europe and in Asia, and equals 60 Hz in North America.

The graph of the power network is described by the tuple $(\mathcal{V}, \mathcal{E})$, where \mathcal{V} is the set of nodes and \mathcal{E} is the set of lines. Denote by $n_{\mathcal{E}}$ the number of lines and by $n_{\mathcal{V}}$ the number of nodes. It is assumed that the undirected graph of the power network is connected, meaning that for every tuple $(\bullet, \triangleright) \in \mathcal{E}$, there exists a path from \bullet to \triangleright .

The power system dynamics is specified by the following equations,

$$\frac{d\theta(t)}{dt} = \omega(t), \quad \theta(0) = \theta_0, \quad (1)$$

$$M \frac{d\omega(t)}{dt} = -D\omega(t) - BW f_d(\theta(t)) + p(t), \quad \omega(0) = \omega_0; \quad (2)$$

$t \in T = [0, +\infty)$, where

$$f_d(\theta) = (\sin(\theta_{i_k} - \theta_{j_k}), \forall k = (i_k, j_k) \in \mathcal{E}) \quad (3)$$

$$= \sin(B^T \theta) \in \mathbb{R}^{n_{\mathcal{E}}}; \text{ which satisfies that,}$$

$$\forall \theta \in \mathbb{R}^{n_{\mathcal{V}}}, \forall \psi \in \mathbb{R},$$

$$f_d(\theta) = f_d(\theta + \psi \times \mathbf{1}_{n_{\mathcal{V}}}); \quad (4)$$

$$M \in \mathbb{R}_{\text{diag}}^{n_{\mathcal{V}} \times n_{\mathcal{V}}}, \forall i \in \mathbb{Z}_{n_{\mathcal{V}}}, M_{i,i} > 0;$$

$$D \in \mathbb{R}_{\text{diag}}^{n_{\mathcal{V}} \times n_{\mathcal{V}}}, \forall i \in \mathbb{Z}_{n_{\mathcal{V}}}, D_{i,i} \geq 0;$$

$$B \in \mathbb{R}^{n_{\mathcal{V}} \times n_{\mathcal{E}}}, L \in \mathbb{R}^{n_{\mathcal{V}} \times n_{\mathcal{V}}}, W \in \mathbb{R}_{\text{diag}}^{n_{\mathcal{E}} \times n_{\mathcal{E}}},$$

$$B_{i,k} = \begin{cases} +1, & \text{if } k = (i, j_k) \in \mathbb{Z}_{n_{\mathcal{E}}}, \\ -1, & \text{if } k = (j_k, i) \in \mathbb{Z}_{n_{\mathcal{E}}}, \\ 0, & \text{else;} \end{cases}$$

$$L_{i,j} = \begin{cases} b_{i,j} \hat{V}_i \hat{V}_j, & \text{if } (i, j) \in \mathcal{E}, \\ 0, & \text{else;} \end{cases}$$

$$W_{k,k} = L_{i_k, j_k} > 0, \quad \text{if } k = (i_k, j_k) \in \mathcal{E};$$

where $b_{i,j} = \frac{1}{i_j} \hat{V}_i \hat{V}_j$ is the effective capacity of line $(\bullet, \triangleright) \in \mathcal{E}$, in which \hat{V}_i is the voltage at node \bullet and i_j is the susceptance of line $(\bullet, \triangleright)$, the dynamics of the voltage is neglected in the short horizon, and i_j is considered as a constant on this horizon.

Call $\theta : \mathcal{J} \rightarrow \mathbb{R}^{n_{\mathcal{V}}}$ the *phase deviation vector*, $\omega : \mathcal{J} \rightarrow \mathbb{R}^{n_{\mathcal{V}}}$ the *frequency deviation vector* (\mathcal{J} are relative to the nominal frequency), $p = [p^+ \triangleright p^-]^T : \mathcal{J} \rightarrow \mathbb{R}^{n_{\mathcal{V}}}$ the *power vector*, $p^+ : \mathcal{J} \rightarrow \mathbb{R}^{n^+}$ the *vector of power supplies*, $p^- : \mathcal{J} \rightarrow \mathbb{R}^{n_{\mathcal{V}} - n^+}$ the *vector of power loads*, $M \in \mathbb{R}_{s+}^{n_{\mathcal{V}} \times n_{\mathcal{V}}}$ the *matrix of inertias*, $D \in \mathbb{R}_{+}^{n_{\mathcal{V}} \times n_{\mathcal{V}}}$ the *matrix of damping constants*, $L \in \mathbb{R}_{+}^{n_{\mathcal{V}} \times n_{\mathcal{V}}}$, the *matrix of power line capacities*, i_d is the index of line $(\bullet, \triangleright_k)$, $B \in \mathbb{R}^{n_{\mathcal{V}} \times n_{\mathcal{E}}}$, the *incidence matrix*, where the directions of the lines are consistently specified, and call $f_d \in \mathbb{R}^{n_{\mathcal{E}}}$ the *vector of sines of the phase-angle differences across power lines*. It is assumed that, for a sufficiently rich subset of initial conditions (not specified in the paper), there exists a unique solution of the differential equation of the power system. Denote by $(\theta(t); \omega(t); 0 > 0) \triangleright (\theta(t); \omega(t); 0 > 0)$ for all times $t \in \mathcal{J}$, the solution of the differential equation where the state at time $t \in \mathcal{J}$ is denoted by $(\theta(t); \omega(t))^T$.

For any power line indexed by $k = (\bullet, \triangleright_k) \in \mathcal{E}$ denote the *phase-angle difference* of that power line and the *power flow* through that power line, both used below, respectively by,

$$\begin{aligned} (\theta_{i_k} - \theta_{j_k}) : \mathcal{J} &\rightarrow \mathbb{R} \\ i_{k,j_k} \sin(\theta_{i_k} - \theta_{j_k}) : \mathcal{J} &\rightarrow \mathbb{R} \end{aligned}$$

The flow of a power line is bounded by the capacity i_{k,j_k} of the line because the absolute value of the sine function is bounded by the real number one.

2.3 The Synchronous State

Consider the nonlinear power system described in Section 2.2. A short while after the start of the short horizon, the electric machines will run steady. One calls such a state a synchronous state rather than a steady state. In the power

network, we suppose a subset of the nodes provide only power supply and a complementary subset have only power demand. The nodes are labeled such that:

$$p(t) = \begin{bmatrix} p^+(t) \\ -p^-(t) \end{bmatrix} \Leftrightarrow p^+(t) = [p_1^+(t) \ \cdots \ p_{n^+}^+(t)]^\top > \\ p^-(t) = [p_{n^++1}^-(t) \ \cdots \ p_{n_V}^-(t)]^\top >$$

which means that the nodes $1 \rightarrow n^+$ have only power supply and the nodes $n^+ + 1 \rightarrow n_V$ have only power demand.

Consider a steady power vector $p_{sp} \in \mathbb{R}^{n_V}$. Recall that $d(\cdot)$ and B are defined with respect to a frame rotating at the nominal frequency. A *synchronous state* is defined as a tuple $(s > s \mathbf{1}_{n_V}) \in \mathbb{R}^{2n_V}$ with $s \in \mathbb{R}$, which satisfy the *synchronous state equations*,

$$0 = -D \mathbf{1}_{n_V} s - B d(s) + p_{sp} > s \mathbf{1}_{n_V} = 0 \Leftrightarrow \quad (5)$$

$$0 = -D_{(i,i)} s - \sum_{j=1}^{n_V} i,j \sin(s_i - s_j) + p_{sp,i} > 0 = s \quad (6)$$

Remark 2.1 *For the purposes of this paper, it is essential that the nonlinear character of the power system is used. Without this nonlinear character, the understanding of the effects of the stochastic fluctuations on the stability of the power system is lost. For a linear direct current (DC) analysis, the readers are referred to [57, Remark 4.1], where it is explained that the linear DC model, in which the sin function is absent from (6), is insufficient for the analysis of the variance of the invariant distribution.*

2.4 The Existence of a Strictly-Stable Synchronous State

Assumption 2.2 *It is assumed that, for the nonlinear power system, there exists a synchronous state $(s > s \mathbf{1}_{n_V})$, which satisfies the condition that $(s_{i_k} - s_{j_k}) \in (-2 > + 2)$, for all $(k > k) \in \mathcal{E}$ and $s = 0$. That state will be referred to as a strictly-stable synchronous state. If a strictly-stable synchronous state exists then it is unique, [43].*

The synchronous state is a solution of the synchronous state equation (5). The solvability of this equation has received much attention in the literature, [4], [21], [10], [43]. Below we use a solution procedure from the literature.

Theorem 2.3 [10]. *Consider the power system specified in 2.2. There exists a unique strictly-stable synchronous state if there exists a $\alpha \in (0 > 2)$ such that,*

$$\|B^\top (B - B^\top)^\dagger p_{sp}\|_\infty \leq \sin(\alpha) \quad (7)$$

Note that $B^\top (B - B^\top)^\dagger p_{sp}$ has been detailed in Appendix 2.1 as a formula $A p_s + \dots$ where A and \dots can be computed from the given line capacities, network incidence matrix and the predicted power demand of next short horizon, and p_s is the decision vector which will be explained in detail later in Section 2.5.

Remark 2.4 *Assumption 2.2 is related to the existence of bifurcations of power systems. The bifurcation scenario of the RTS 96 network is introduced on page 13 of the supporting information of [10]. In a recent publication [22], the authors localize the solutions in each winding cell, and they claimed and proved that there is at most one solution in each wind cell. However, there still exist cases where no solution can be found. Hence the above assumption is motivated.*

2.5 The Domain of the Power Supply Vector

Definition 2.5 The domain of the power supply vector.

Consider the maximal available power supply and the power demand for the next short horizon, denoted respectively by $p^{+,max} \in \mathbb{R}_+^{n^+}$ and $p^- \in \mathbb{R}_{sum}^{n^-}$. Define then $p_{sum}^{+,max} = \sum_{i=1}^{n^+} p_i^{+,max}$ and $p_{sum}^- = \sum_{i=1}^{n^-} p_i^-$. It is assumed that $p_{sum}^{+,max} \geq p_{sum}^-$. Note that p_{sum}^- is strictly positive.

Construct a power supply vector $p^+ \in \mathbb{R}^{n^+}$ according to the following steps,

- (1) choose $p_{sum}^+ \in \mathbb{R}$ such that $p_{sum}^+ = p_{sum}^-$
- (2) choose $p_i^+ \in [0, p_i^{+,max}] \forall i = 1, 2, \dots, n^+ - 1$

$$\text{and set } p_{n^+}^+ = p_{sum}^+ - \sum_{i=1}^{n^+-1} p_i^+;$$

- (3) p^+ has to satisfy that $\forall i \in \mathbb{Z}_{n^+}$

$$p_{sum}^+ - \sum_{i=1, i \neq j}^{n^+} p_i^+ \in [0, p_j^{+,max}]$$

The latter conditions denote that: (1) the power supply of p^+ equals the power demand; (2) the power supply components $p_1^+, p_2^+, \dots, p_{n^+-1}^+$ are feasible; (3) the power supply vector p^+ satisfies these conditions.

Define the decision vector as a subvector of the power supply vector, by the formula

$$p_s = [p_1^+ \quad p_2^+ \quad \dots \quad p_{n^+-1}^+] \in \mathbb{R}^{n^+-1}.$$

Define the domain of the feasible vector as the set \mathcal{D}^+ , where the matrices A_1, A_2 are provided in .1.3,

$$\begin{aligned} \mathcal{D}^+ &= \{ p^+ \in \mathbb{R}^{n^+} \mid p^+ \in [p^+, p^{+,max}] \} \\ &= \left\{ p_s \in \mathbb{R}_+^{n^+-1} \mid \text{conditions (1), (2), (3) above} \right. \\ &\quad \left. \text{all hold, then we can derive } A_1 p_s \geq p_s \leq A_2 \right\} \end{aligned}$$

Condition (1) that power supply p_{sum}^+ equals power demand p_{sum}^- and that the synchronous state equation (5) holds, imply that the synchronous frequency ω_s equals zero.

Proposition 2.6 *The domain \mathcal{D}^+ is compact and convex. Moreover, it is a polytope.*

2.6 Linearize the Nonlinear Power System

The procedure to linearize the deterministic nonlinear power control system at a strictly-stable synchronous state may be found in the references [62] and [38].

$$\frac{dp(t)}{dt} = J(\theta_s) p(t) + \begin{bmatrix} 0 \\ I \end{bmatrix} \Delta p(t) \quad (8)$$

$$p(0) = \begin{bmatrix} p(0) - p_{sp} \\ 0 \end{bmatrix} \Delta p(t) = p(t) - p_{sp}$$

$$p(t) = \begin{bmatrix} \Delta p(t) \\ p(t) \end{bmatrix} = \begin{bmatrix} p(t) - p_{sp} \\ p(t) \end{bmatrix}$$

$$J(\theta_s) = \begin{bmatrix} 0 & I_{n\nu} \\ -B^{-1} & F(\theta_s) - D^{-1} \end{bmatrix} \quad (9)$$

$$F(\theta_s) = \left(\frac{d(\cdot)}{d\theta} \right) \Big|_{\theta=\theta_s} \in \mathbb{R}^{n\nu \times n\nu}$$

where the matrix of equation (9) is called the *Jacobian matrix* and the product $B^{-1} F(\theta_s)$ is called the *Laplacian matrix* of the power network. The Laplacian matrix depends on the synchronous state considered. The reader finds in Appendix .1.1 the Laplacian matrix of a complete power network. In general, if the synchronous state is such that the phase-angle difference is closer to either $+\pi/2$ or to $-\pi/2$, the closer the modulus of the eigenvalues of $J(\theta_s)$ will be to zero.

The Laplacian matrix of the power network is in general a singular matrix, [53]. For all of the examples of Section 4 the Laplacian matrix has precisely one eigenvalue at zero. The eigenvalues of the Jacobian matrix of a power system for a *complete* power network, are discussed in [43, 61].

2.7 The Stability of a Nonlinear Power System

The reader finds in this subsection the concepts of the domain of attraction of a synchronous state and the definition of transient stability of a power system. For concepts and a classification of power system stability, see [26, 27]. The main basis for this subsection are the papers on stability of nonlinear power systems, [62] and [6].

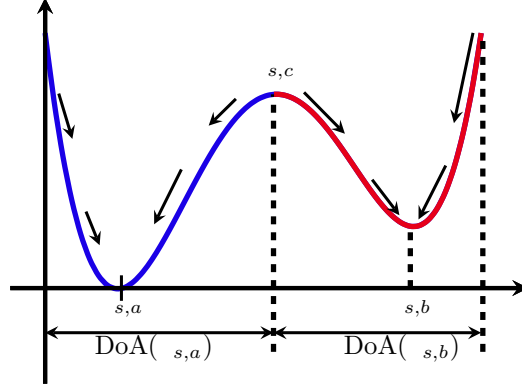


Figure 1: Two stable points s,a and s,b with their domain of attraction and a saddle point s,c

Definition 2.7 Define the domain of attraction of a strictly-stable synchronous state, $(s > s \times 1_{n_V}) \in \mathbb{R}^{2n_V}$, of a deterministic nonlinear power system as a subset of the state set such that the state trajectory of the power system, starting at any state of this subset, will converge to the considered synchronous state; in terms of mathematical notation,

$$\text{DoA}(s > s) = \left\{ \begin{array}{l} (s_0 > s_0) \in \mathbb{R}^{2n_V} \\ \lim_{t \rightarrow +\infty} (s(t; s_0 > s_0)) = (s > s \times 1_{n_V}) \end{array} \right\}$$

Call the dynamic behavior of the power system at the strictly-stable synchronous state s transient stable if (1) $(\text{spec}(J(s > s)) \setminus \{0\}) \subset \mathbb{C}^-$ and (2) the state trajectory, when started inside the open domain, remains inside the domain during the entire horizon.

An example with domains of attraction is displayed in Fig. 1. The figure displays an abstract energy function as a function of a one-dimensional state. Displayed are the open domains of attraction of the two steady states s,a and s,b and the steady state s,c whose domain of attraction is only the steady state itself.

In the literature, there are necessary and sufficient conditions for stability of the synchronous state of a deterministic nonlinear power system, which is often condition (1) of transient stability. A reference for these conditions is the paper of J. Zaborszky et al., [61] in which also monitoring of a power system is described.

Which concept of stability is needed for a *deterministic nonlinear power system* when it is subjected to either a single disturbance or a sequence of deterministic disturbances, not specified in the nonlinear power system? Then the state trajectory of such a system may return to the synchronous state or will fluctuate in the domain of attraction near the synchronous state. However, due to particular disturbances, the state trajectory may leave the domain of attraction and move into the domain of another synchronous state where its dynamic behavior may be different. There are no concepts for this form of instability, caused by deterministic disturbances of power systems. The reader is referred to the papers [62], [6] for this dynamic behavior. A departure from the domain of a synchronous state is best avoided by a form of control.

In the remainder of the paper a necessary condition for the transient stability of a power system will be used.

Definition 2.8 The deterministic nonlinear power system will be said to be phase-angle-difference stable if the phase-angle differences of all power lines remain in the safe subset $(-\pi/2 > +\pi/2) \subset \mathbb{R}$ for all times. If a power system is no longer phase-angle-difference stable then one says that the power system has lost synchronization.

The domain of attraction of a state set is difficult to compute. Hence the use of the subset $(-\pi/2 > +\pi/2) \subset \mathbb{R}$ for the phase-angle differences of any power line. The literature on the relation of a safe subset of the phase-angle differences to that of the domain of attraction of a synchronous state, including stability of a deterministic power system, includes the following: [43], [63], [61] and [50, Lemma 5.2].

There is no proof in the literature that the phase-angle-difference stability implies that the state of the power system remains in the domain of attraction of a synchronous state.

The phase-angle differences between buses have been widely used as a measure of the transient stability of power systems in the literature. See [58] for the escape probability of the phase-angle differences from the set $(-\pi, \pi)$ as a metric for transient stability of a stochastic power system. A phase plane of high-order derivatives of angle difference for a Single Machine Infinite Bus System is plotted in [31] through which the unstable equilibrium can be found, and the transient stability can thus be evaluated. In [45], the line whose phase-angle difference is inside the domain $(-\pi, \pi)$ is used as a critical line for the investigation of the small-disturbance rotor stability of power systems.

2.8 The Stochastic Linearized Power System

A stochastic power system is formulated based on the linearization of the deterministic nonlinear power system. The deterministic functions (\cdot) become stochastic processes in the stochastic system defined below. The process Δp is below defined as a Brownian motion process. It denotes the difference of the power supply and the power demand, each of which as a difference from their values at the synchronous state on a short horizon. Here, we refer to [8], where the uncertainty of the load is modeled as a Brownian motion. The *stochastic linearized power system* is then defined by the linear stochastic differential equation, [24], [30],

$$\dot{x}(t) = J(x(t))x(t) + K v(t) \quad (10)$$

$$\dot{x}(t) = C x(t) \quad (11)$$

$$: \Omega \times \mathcal{J} \rightarrow \mathbb{R}^{2n_v} \quad : \Omega \times \mathcal{J} \rightarrow \mathbb{R}^{n_\varepsilon}$$

$$x(0) = \begin{bmatrix} x_1(0) \\ x_2(0) \end{bmatrix} \in \mathbb{R}^{2n_v \times n_v}$$

$$C = \begin{bmatrix} B^T & 0 \end{bmatrix} \in \mathbb{R}^{n_\varepsilon \times 2n_v}$$

where $(\Omega, \mathcal{F}, \mathbb{P})$ denotes a probability space consisting of a set Ω , a \mathcal{F} -algebra \mathcal{F} , and a probability measure \mathbb{P} ; $\mathcal{J} = [0, \infty)$ denotes the time index set; $x(0) : \Omega \rightarrow \mathbb{R}^{2n_v}$ denotes the initial state of the stochastic system which is assumed to have a Gaussian distribution with expectation $x(0) \in \mathbb{R}^{2n_v}$ and a symmetric positive-definite variance matrix $\Sigma_{x(0)} \in \mathbb{R}^{2n_v \times 2n_v}$, hence $x(0) \in G(x(0), \Sigma_{x(0)})$; $v : \Omega \times \mathcal{J} \rightarrow \mathbb{R}^{n_\varepsilon}$ denotes a Brownian motion process such that $\forall s > t \in \mathcal{J}, v(t) - v(s) \in G(0, (t-s)I_{n_\varepsilon})$, while $\mathcal{F}^{x(0)}, \mathcal{F}^v$ are independent \mathcal{F} -algebras; $K_2 \in \mathbb{R}^{n_\varepsilon \times n_\varepsilon}$ denotes a matrix which multiplies the vector-valued Brownian motion, which is a diagonal matrix with $K_2(i, i) \geq 0, i \in \mathbb{Z}_{n_\varepsilon}$.

2.9 Stochastic Stability of a Stochastic Power System

Stochastic stability of nonlinear stochastic systems is extensively treated in the literature, [19, 25, 28, 29, 35]. The main concept is the invariant probability distribution of the state of the system and its properties. For the characterization of stochastic linearized power system considered, (10, 11), attention will be focussed on the variance of the vector of phase-angle differences.

Definition 2.9 Consider the stochastic linearized power system (10, 11), and consider a synchronous state $x_s = (x_s, x_{n_v})$ which satisfies Assumption 2.2. Define the safe set X_c of the phase-angle differences as a subset of \mathbb{R}^{2n_v} by the formulas,

$$\Theta_c = \left\{ x \in \mathbb{R}^{2n_v} \mid \forall i, j \in \mathbb{Z}_{n_v}, x_i - x_j \in (-\pi, \pi) \right\}$$

$$X_c = \Theta_c \times \mathbb{R}^{n_\varepsilon} \subset \mathbb{R}^{2n_v}$$

Call the phase-angle differences of a power system at the strictly-stable synchronous state x_s during a short horizon and for a prespecified value $\alpha \in (0, 1)$, (probabilistically) safe-stable (1) if $\text{spec}(J(x_s)) \setminus \{0\} \subset \mathbb{C}_\alpha^-$, and (2) if the stochastic power system is started at the synchronous state, then the probability is higher than $(1 - \alpha) \in (0, 1)$ that the phase-angle differences, remain inside the safe set $X_c = \Theta_c \times \mathbb{R}^{n_\varepsilon}$ during the considered horizon.

In this paper attention is focused on a stochastic linearized power system and a strictly-stable synchronous state such that the phase-angle differences of all power lines are safe-stable. This condition implies that synchronization of the power system is maintained.

2.10 The Invariant Distribution of the Stochastic Linearized Power System

It follows from [24, Theorem 6.17] and [30, Theorem 1.52] that the stochastic processes $x(t)$ and $y(t)$ of the stochastic linearized power system (10, 11) are Gaussian processes with for all times $t \in \mathcal{J}$, $(x(t), y(t)) \in G(x(t), y(t))$ and $(t) \in G(y(t), x(t))$.

If the Jacobian matrix $J(s, \theta)$ is Hurwitz, hence $\text{spec}(J(s, \theta)) \subseteq \mathbb{C}_o^-$, the following properties of the mean value and the variance matrix hold,

$$\begin{aligned} 0 &= \lim_{t \rightarrow \infty} x(t) & 0 &= \lim_{t \rightarrow \infty} y(t) \\ \bullet_x &= \lim_{t \rightarrow \infty} \bullet_x(t) & \bullet_y &= \lim_{t \rightarrow \infty} \bullet_y(t) \end{aligned}$$

and where \bullet_x is the unique solution of the following Lyapunov equation and \bullet_y satisfies,

$$0 = J(s, \theta) \bullet_x + \bullet_x J(s, \theta)^\top + K K^\top \quad (12)$$

$$\bullet_y = C \bullet_x C^\top \quad (13)$$

But in fact, the system matrix $J(s, \theta)$ is not Hurwitz because the Laplacian matrix $B - F(s)$ has a zero eigenvalue.

The reader finds in [53] a discussion for the determination of the variances of the power lines based on an eigenvalue decomposition and a reduction process.

In control engineering, the system operators want to determine that power line which is the most vulnerable for instability. Hence there is a need to compute the variances of the phase-angle differences of all power lines. The H_2 norm of the input-output LTI system is insufficient for the computation of the variance due to high computational complexity, see [53].

Assumption 2.10 Consider a stochastic linearized power system (10, 11), where the nonlinear power system has been linearized at a strictly-stable synchronous state.

- (1) Assume that the diagonal matrix K has strictly-positive diagonal elements, hence, for all $k \in \mathcal{V}$, $K_{k,k} < 0$.
- (2) $(J(s, \theta) > K)$ is a controllable pair.

Condition (1) of Assumption 2.10 and the fact that, in the graph associated with the system with nodes at states and inputs, there exists a path from any node representing a frequency to a node with a disturbance, imply that Condition (2) of Assumption 2.10 holds, [7].

Proposition 2.11 Consider a stochastic linearized power system (10, 11). Assume that either Condition (1) or Condition (2) of Assumption 2.10 holds. Then, for any power line $k \in \mathbb{Z}_{n_\epsilon}$ and any fixed power supply vector $p_s \in \mathbb{R}^+$, the standard deviation $\mathfrak{g}_k(p_s)$ is strictly positive; in terms of notation, $\mathfrak{g}_k(p_s) = (\bullet_{y,(k,k)})^{1/2} < 0$.

The proof of the above proposition may be found in Appendix .1.2.

From the discussion above follows that the random variable of the phase-angle difference over power line k of the power network, $i_k(t) - j_k(t)$, has the invariant Gaussian probability distribution, $\forall t \in \mathcal{J}$ and $\forall (p_s) \in \mathcal{E}$,

$$\begin{aligned} i_k(t) - j_k(t) &\in G(k(p_s) > \mathfrak{g}_k^2(p_s)); \\ k(p_s) &= s_{i,k}(p_s) - s_{j,k}(p_s) > \\ \mathfrak{g}_k(p_s) &= \bullet_{y,(k,k)}(p_s)^{1/2} < 0; \text{ then,} \\ \frac{i_k(t) - j_k(t) - k(p_s)}{\mathfrak{g}_k(p_s)} &\in G(0 > 1); \\ &= \int_{-\infty}^{r_\epsilon} p_{G(0,1)}(w) \, w \end{aligned}$$

See Table 1 for the relation between the threshold values and the values of the parameter, (r_ϵ) , of $G(0 > 1)$.

2.11 An Upper Bound

The probabilities that the maximum of a stationary Gaussian process on a finite interval is larger than a particular threshold, are available in the literature, see for example [15, Section 6.5]. However, even for a Brownian motion process the probabilities are expressed as an infinite series of integrals over Gaussian density functions. Such expressions

	r_ϵ
0.050	-1.65
0.040	-1.76
0.030	-1.89
0.020	-2.06
0.010	-2.33
0.001	-3.08

Table 1: Relation of probabilities and thresholds of a Gaussian probability distribution with mean zero and variance one. Thus, if $\epsilon \in G(0,1)$ and $r_\epsilon \in (0,1)$ then $\mathbb{P}(\{x \leq r_\epsilon\}) \leq \epsilon$ and r_ϵ is an approximation of the maximal such real number.

require approximations which are computationally intensive. Therefore it has been decided to restrict attention to the probability at a particular time that the process exits the safe set according to the invariant probability distribution.

Proposition 2.12 *Consider the stochastic linearized power system.*

(a) *The probability that the power flow of any power line exits the safe set according to the invariant distribution of the vector of power line flows, satisfies,*

$$\begin{aligned}
& \forall \epsilon \in \mathbb{Z}_{n_\epsilon} \forall p_s \in P^+ \\
& p_{out,k}(p_s) \\
& = (\mathbb{P}(\{x \in \Omega \mid i_k(x) - j_k(x) \leq -2\}) + \\
& \quad + (\mathbb{P}(\{x \in \Omega \mid i_k(x) - j_k(x) \geq +2\})) \\
& = G(0,1)(r_{a,k}(p_s)) + G(0,1)(-r_{b,k}(p_s)) \\
& \leq 2 G(0,1)(r_{a,b,k}(p_s)) \\
r_{a,k}(p_s) & = \frac{-2 - i_k(p_s)}{g_k(p_s)} \\
-r_{b,k}(p_s) & = \frac{-2 + j_k(p_s)}{g_k(p_s)}; \\
r_{a,b,k}(p_s) & = \max\{r_{a,k}(p_s), -r_{b,k}(p_s)\} \\
r_{a,b,k}(p_s) & = \frac{-2 + |i_k(p_s)|}{g_k(p_s)}
\end{aligned}$$

(b) *An upper bound. If $r_{a,b,k}(p_s) \leq r_{\epsilon/2}$ then $p_{out,k}(p_s) \leq \epsilon$.*

Infimization of the lower bound derived above leads to the following alternative optimization criteria,

$$\begin{aligned}
& (a) \inf_{p_s \in P^+} \max_{k \in \mathbb{Z}_{n_\epsilon}} r_{a,b,k}(p_s) \\
& = \inf_{p_s \in P^+} \max_{k \in \mathbb{Z}_{n_\epsilon}} \left(\frac{-2 + |i_k(p_s)|}{g_k(p_s)} \right); \\
& (b) \inf_{p_s \in P^+} \max_{k \in \mathbb{Z}_{n_\epsilon}} \left(\frac{|i_k(p_s)|}{g_k(p_s)} - r_\epsilon \right) \\
& = \inf_{p_s \in P^+} \max_{k \in \mathbb{Z}_{n_\epsilon}} \left(\frac{|i_k(p_s)| - r_\epsilon g_k(p_s)}{g_k(p_s)} \right); \\
& (c) d^* = \inf_{p_s \in P^+} \max_{k \in \mathbb{Z}_{n_\epsilon}} [|i_k(p_s)| - r_\epsilon g_k(p_s)] \\
& \text{where } r_\epsilon \in (-\infty, 0)
\end{aligned}$$

Below optimization criterion (c) will be used. The criteria (a) and (b) involve division by g_k which involves computational issues that are best avoided.

Note that $d^* < -2$ with a parameter r_ϵ implies that there exists a supply vector $p_s \in P^+$ such that $p_{out}(p_s) \leq 2 - r_\epsilon$. The proof of this proposition can be found in Appendix .1.4.

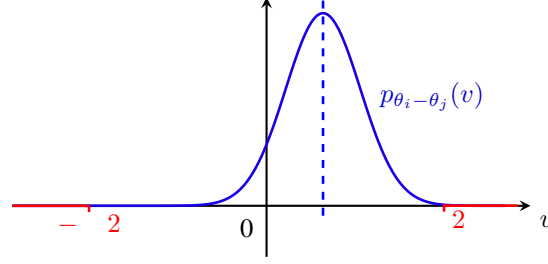


Figure 2: The probability density function of the phase-angle difference $(\theta_{i_k} - \theta_{j_k})$ of the power flow in power line $(i_k, j_k) \in \mathcal{E}$; and two red bars for the probabilities that the phase-angle difference is larger than $+2$ or less than -2 . The parameters of the probability density function displayed are $(\mu, \sigma) = (0.4995, 0.3344)$ which values are chosen identical to those of Fig. 7 for ‘without control’.

2.12 A Sequence of Short Horizons

Recall that the *time index set*, also called the *horizon*, is the set of the positive real numbers $\mathcal{J} = [0, +\infty)$. This time index set is now partitioned into an infinite sequence of *short horizons* all of the same length, for example 3 or 5 or 15 minutes, as is done in discretization of a continuous-time system.

3 The Control Problem

3.1 The Setting of the Control Problem

Consider the nonlinear power system and the stochastic linearized power system both defined in the previous section. Consider the time index $\mathcal{J} = \mathbb{R}_+$ partitioned into an infinite sequence of short horizons. It is assumed that, during any short horizon, there is available to the controller a prediction of the total power demand \hat{p}_{sum}^- of the power system in the next short horizon which is based on output feedback measurements.

The problem to be investigated and formalized below is to compute, during any short horizon, an input for the next short horizon in the form of a vector p^+ of power supplies for all nodes with power supply. That constant input is then used during the entire next short horizon.

The computation of the vector p^+ of power supplies proceeds as described in Subsection 2.5. but with the power demand of the next short horizon replaced by a prediction of that power demand. Set first $p_{sum}^+ = \hat{p}_{sum}^-$, thus total power supply equals the prediction of total power demand. Secondly, determine the vector $p_s = \{p_1^+, p_2^+, \dots, p_{n^+-1}^+\}$ according to the optimization problem *described below* and satisfying the conditions (1)-(3) of Subsection 2.5.

The approach of control sketched above, is a generalization of secondary frequency control, [11, 12, 32, 59]. In the quoted papers, one computes the vector $p_s = \{p_1^+, p_2^+, \dots, p_{n^+-1}^+\}$ to *minimize a cost function based only on the economic cost*.

The main difference of the approach proposed in this paper compared with classical secondary frequency control, is therefore the cost criterion for the determination of the components of the vector of power supplies.

The term *control problem* is preferred by the authors over the term *optimization problem*. It is stated by P. Kundur in his book, [26, Subsec. 11.1.6, p. 617], that the controllers of a power system have available very recent information of line flows, system frequencies, and MW power loadings for automatic generation control. Thus secondary frequency control is based on output feedback. From the observations one has to compute a prediction for the power demand in the next future horizon. In this paper it is assumed that the control computer of a power system can compute such a prediction, hence the control is based on output feedback.

The problem formulated is a problem of *stochastic control theory*. The analytic form of the stochastic control problem is nonlinear due to the optimization criterion of the probabilities of exiting the safe subset. In the research areas of communication networks and of motorway control, there are treated stochastic control problems with a finite-capacity of network lines and a probability of exceeding a safe subset, [44, 52].

Fig. 2 illustrates the stochastic control problem. The extremal probabilities of power line that $(\theta_{i_k} - \theta_{j_k}) < +2$ and $(\theta_{i_k} - \theta_{j_k}) < -2$ are to be made sufficiently small by a choice of the power supply vector.

3.2 The Control Objective Function

Definition 3.1 The control objective function.

Consider the stochastic linearized power system of Section 2.8. Define the functions,

$$\begin{aligned} \forall (s, k) \in \mathbb{Z}_{n_{\mathcal{E}}} \times \mathbb{Z}_{n_{\mathcal{E}}} \times \mathbb{Z}_{n_{\mathcal{E}}} \times \mathbb{Z}_{n_{\mathcal{E}}} \\ a_{s,k}(p_s) &= |s, i_k(p_s) - s, j_k(p_s)| \\ &= \arcsin(|(A p_s + \theta)_k|) = |k(p_s)| \end{aligned} \quad (14)$$

$$g_k(p_s) = a_{s,k}(p_s) + r_{\epsilon} \theta_k(p_s) \in \mathbb{R}_{+} \quad (15)$$

$$f(p_s) = \|(g_k(p_s))\|_{\infty} = \max_{k \in \mathbb{Z}_{n_{\mathcal{E}}}} g_k(p_s) \quad (16)$$

$$a_{s,k} : \mathbb{R}_{+}^{n_{\mathcal{E}}} \rightarrow \mathbb{R}_{+} \quad a_s : \mathbb{R}_{+}^{n_{\mathcal{E}}} \rightarrow \mathbb{R}_{+}^{n_{\mathcal{E}}}$$

$$g_k : \mathbb{R}_{+}^{n_{\mathcal{E}}} \rightarrow \mathbb{R}_{+} \quad \theta_k : \mathbb{R}_{+}^{n_{\mathcal{E}}} \rightarrow \mathbb{R}_{+} \quad r_{\epsilon} \in \mathbb{R}_{+}$$

$f(p_s)$ is the maximum over all power lines of an upper bound on the probability that the power flow of any power line is outside the safe set, when the power supply vector is $p_s \in \mathbb{R}_{+}^{n_{\mathcal{E}}}$. f can be considered to be the *control objective function*. The parameter $r_{\epsilon} \in \mathbb{R}_{+}$ which appears in (15) is a parameter of the control objective function. Appendix 2.1 contains the formulas of the matrices A and θ of $a_{s,k}(p_s)$ in (14).

For a particular decision vector $p_s \in \mathbb{R}_{+}^{n_{\mathcal{E}}}$, $f(p_s)$ can be computed by the following steps: (1) For the given power network parameters, compute A and θ of $a_{s,k}(p_s)$ according to Appendix 2.1 which is also addressed in 2.4 and determine the synchronous phase-angle differences vector $s, i_k - s, j_k = \arcsin(A p_s + \theta) \in (-\pi/2, \pi/2)^{n_{\mathcal{E}}}$. Then compute $|k(p_s)|$ for all $k \in \mathbb{Z}_{n_{\mathcal{E}}}$. (2) Compute $F(p_s > 0)$ and the Jacobian matrix $J(p_s > 0)$. (3) Using the matrices $(J(p_s > 0) > K > C)$ and a reduction process, solve a Lyapunov equation, and then compute θ_y and $\theta_k(p_s)$ for all $k \in \mathbb{Z}_{n_{\mathcal{E}}}$; and (4) compute $f(p_s)$ according to the equations (14,15,16).

3.3 The Control Problem

Problem 3.2 Control of the probability that any phase-angle difference of a power line leaves the safe subset.

Consider the stochastic linearized power system described by the equations (10, 11) and a value $a \in (0, 1)$.

The control problem is to determine a vector of power supplies for the next short horizon, such that the probability mentioned above, is less than the value a . Furthermore, that probability is best minimized.

In terms of a mathematical formula, the problem is to solve the following optimization problem, including to determine a minimizer $p_s^* \in \mathbb{R}_{+}^{n_{\mathcal{E}}}$ and a value $a \in \mathbb{R}$, according to,

$$\begin{aligned} a &= f(p_s^*) = \inf_{p_s \in P^+} f(p_s) \\ &= \inf_{p_s \in P^+} \max_{k=(i_k, j_k) \in \mathcal{E}} \left[|s, i_k(p_s) - s, j_k(p_s)| + r_{\epsilon} \theta_k(p_s) \right] \end{aligned}$$

If the value satisfies $a < 2$ then there exists an input vector $p_s \in \mathbb{R}_{+}^{n_{\mathcal{E}}}$ such that the probability is less than a that the phase-angle difference of any power flow leaves the safe subset during a short horizon.

It is proven in a companion paper, [55], that the control objective function defined above, is nondifferentiable and nonconvex. The nondifferentiable property is caused by the absolute value operator in the $a_{s,k}$ in (14), and the infinity norm in (16). The nonconvexity is due to the variance $\theta_k(p_s)$ in (15). A minimizer of the control objective function over the set of power supply vectors exists and an iterative procedure based on a generalized subgradient or first directional derivative produces an approximation sequence which is proven to converge to a rather good local minimizer in a finite number of steps.

After applying the proposed procedure, the determined power supply vector makes the power system relatively more stable with as consequence that the most vulnerable line, (the line with the highest exit probability from the safe set), has a probability to leave the safe subset, below the preset bound. Hence the transient stability of the power system is improved.

4 The Performance of the Controlled Power System for Three Examples

Example 4.1 has been chosen because it has been used to illustrate the Braess paradox. This phenomenon concerns the power flows when scheduling or planning the operations of a power system. Such functions influence the transient

stability of the power system, [56]. Example 4.4 of a ring network has been chosen because such rings often occur in power networks. Example 4.5 of a Manhattan grid has been chosen because it was expected to be relatively stable. For all three examples, the value of the parameter r_ϵ of the control objective function is chosen to be 3.08, which leads to a probability of 99.8% of the power flow inside the safe set.

The reader finds the details of the computations of the examples in a report, [54].

Note that, if one assumes that the probabilities of leaving the safe set are independent and that one is willing to accept a probability of leaving the safe set once per year, then the probability of leaving the safe set in a three minute period may be approximated by $6 \times 10^{-6} \approx ((60 \cdot 3) \times 24 \times 365)^{-1}$.

Of interest to control is the comparison of the performance of a power system *with control*, as proposed in this paper, and a power system *without control*.

Define the *proportional control law* for the power supply vector by the following procedure for a short horizon. Consider the vector of maximal available power supply $p^{+,max}$ and the vector of power demands p^- which satisfy that $\sum_{i=1}^{n^+} p_i^{+,max} = p_{sum}^{+,max} \geq p_{sum}^- = \sum_{j=1}^{n^-} p_j^-$. Choose $p_{sum}^+ = p_{sum}^-$ hence power supply equals power demand. Define the fraction $s = p_{sum}^+ / p_{sum}^{+,max} \in (0,1)$. Define then the power vector $p^+ \in \mathbb{R}^{n^+}$, $p_i^+ = s \times p_i^{+,max}$ for all $i \in \mathbb{Z}_{n^+}$. Then $\sum_{i=1}^{n^+} p_i^+ = p_{sum}^+ = p_{sum}^-$.

The comparison between *without control* and *with control* will then be focused on the three values of,

$$\{(|i_k - j_k| > \theta_k \mid p_s) = |i_k - j_k| + r_\epsilon \theta_k \mid \forall \in \mathcal{E}\}$$

The results of this comparison are displayed below for the examples of a ring network and of a Manhattan grid.

Example 4.1 A particular eight-node power network.

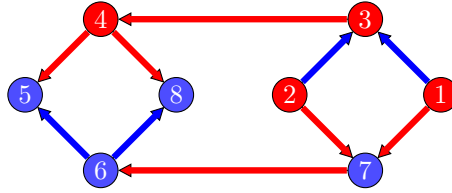


Figure 3: A particular eight-node academic example

This academic power network is borrowed from the paper [56]. It is often used to illustrate the Braess paradox. The network is displayed in Fig. 3, where the nodes which are colored red, 1, 2, 3, 4, provide power supply while nodes which are colored blue, 5, 6, 7, 8, have only power loads.

The parameters of the power system are the inertias, the damping coefficients, the standard deviations of the disturbances, the maximal power supplies and the power demands, and the line capacities. In a second part of the example for other cases, the parameter values are changed to different values. One computation of the first part is displayed in

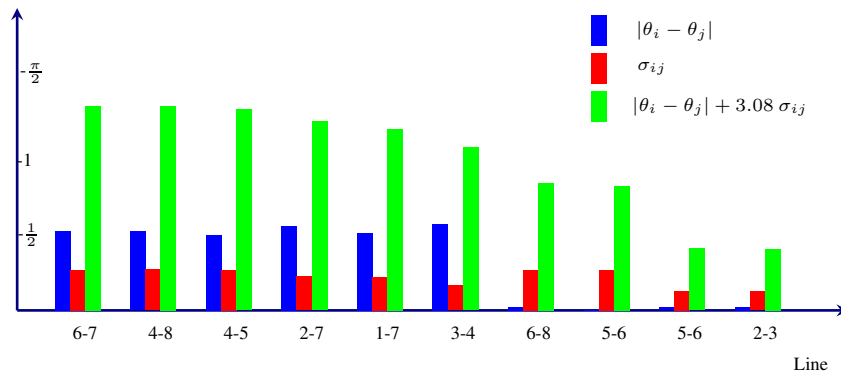


Figure 4: The outputs of the particular eight-node academic network

Fig. 4. The columns of that column chart are ordered according to the values of $|i - j| + 3.08 \rho_{ij}$ in the decreasing order of magnitude.

The conclusions for this example are:

1. There are six lines with relatively high power flows which are colored red and four lines with relatively low power flows which are colored blue in Fig. 3.
2. The computation has been additionally evaluated by discretizing the domain of the power supply vectors for each dimension into a grid with 150 steps. The minimum value computed by this grid method is 1.3529 which is smaller than the value in Table 2 while the time for computation is longer than that of our proposed method.
3. From different initial states, the local minimizers of the control objective function might be different, and that is due to the non-convexity property of the control objective function, see the Tables 2 and 3.
4. It is very amazing that different minimizers have almost the same minimum values, see the minimum values in Tables 2 and 3. Due to this phenomenon, other economic considerations can decide the "best" power injection among these safe ones.

Remark 4.2 A Braess paradox of Example 4.1. If one adds to the power network the line (2-4) between node 2 and node 4 or if one doubles only the capacity of line (3-4) then one expects that the value of the minimum will decrease. Yet, the value of the minimum increases, see the Tables 4 and 5 in contrast with Table 2. This is a paradoxical phenomenon, see the Braess paradox described in [14] and [46].

Remark 4.3 Dealing with a contingency which often happens in power systems. When large power consumers like steel factories or data centers start to work, the power demand increases immediately. Consider the case that the maximal available power supply cannot meet the power demand. By a summation of equation (6) over all nodes, we can get $s = \frac{\sum_{i=1}^{n_V} p_{sp,i}}{\sum_{i=1}^{n_V} D_{(i,i)}}$, thus $s < 0$ and there is a need of load shedding. Consider the case that the maximal available power supply can still meet the power demand, but the amount of the power demand approaches the power supply, the computation result of our proposed procedure is shown in Table 6, while the comparison of with and without control is shown in Table 7. Furthermore, the tail probability computed according to Table 7 is shown in Table 8.

Note that $a_{i,k} = (\omega \in \Omega \mid i_{k,j_k}(\omega) < -2)$, $b_{i,k} = (\omega \in \Omega \mid i_{k,j_k}(\omega) < 2)$, and $p_{out,k}$ is the exit probability computed by our proposed criterion, and it equals two times an upper bound of $a_{i,k}$ and $b_{i,k}$. From these comparison, one can see indeed the power system is more stable after control in a practical sense.

Table 2: Example 4.1. The minimum value and the optimal power vector from the initial power supply vector [12-12-12].

Minimum	p_1	p_2	p_3	p_4
1.3530	11.7679	13.7632	13.5247	10.9441
	p_5	p_6	p_7	p_8
	-12	-12	-13	-13

Table 3: Example 4.1. The minimum value and the optimal power vector from the initial power supply vector [11-11-14].

Minimum	p_1	p_2	p_3	p_4
1.3532	11.7085	12.6649	15.2572	10.3694
	p_5	p_6	p_7	p_8
	-12	-12	-13	-13

Table 4: Example 4.1. Added is line 2 – 4. Results of the minimum value and the optimal power vector from the initial power supply vector [12-12-12].

Minimum	p_1	p_2	p_3	p_4
1.3953	12.0000	14.0000	16.0000	8.0000
	p_5	p_6	p_7	p_8
	-12	-12	-13	-13

Table 5: Example 4.1. Change doubling the capacity of Line 3 – 4. Results of the minimum and the optimal power vector from the initial power supply vector $[12 \ 12 \ 12]$.

Minimum	p_1	p_2	p_3	p_4
1.3712	12.0000	14.0000	16.0000	8.0000
	p_5	p_6	p_7	p_8
	-12	-12	-13	-13

Table 6: Increase the power demand to 59, where the maximal power demand is 60, the minimum value and optimal power vector start from the power supply vector is $[5 \ 5 \ 5]$

Minimum	p_1	p_2	p_3	p_4
1.5306	12.0001	14.001	16.0000	16.9998
	p_5	p_6	p_7	p_8
	-16	-13	-14	-16

Table 7: Example 4.1 The particular eight-node network. Increasing the power demand to almost the maximal power supply, comparison of performance without and with control.

Nodes		Control	$ i_k - j_k $	θ_k	$ i_k - j_k + r_\epsilon \theta_k$
k	k				
4	5	without	0.6746	0.2801	1.5373
4	5	with	0.6687	0.2798	1.5306
4	8	without	0.6746	0.2796	1.5358
4	8	with	0.6687	0.2793	1.5291
6	7	without	0.5834	0.2727	1.4234
6	7	with	0.5944	0.2734	1.4366
2	7	without	0.6127	0.2272	1.3126
2	7	with	0.6187	0.2276	1.3198

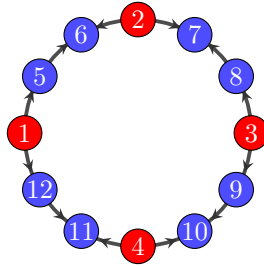


Figure 5: A ring network

Example 4.4 A ring network with twelve nodes. The power network shown in Fig. 5 consists of a ring with four

Table 8: The exit probabilities per component of the vector of phase-angle differences for the two sides of the safe subset of the particular eight-node network according to Table 7, both without control and with control.

Power line	Without control probabilities		With control probabilities		
	a,k	b,k	a,k	b,k	$p_{out,k}$
4-5	5.44e-16	6.88e-04	6.03e-16	6.32e-04	$2 \times 6.33e-04$
4-8	4.84e-16	6.75e-04	5.36e-16	6.19e-04	$2 \times 6.32e-04$
6-7	1.47e-04	1.40e-15	1.78e-04	1.19e-15	$2 \times 6.25e-04$
2-7	3.61e-22	1.24e-05	3.29e-22	1.44e-05	$2 \times 5.64e-04$

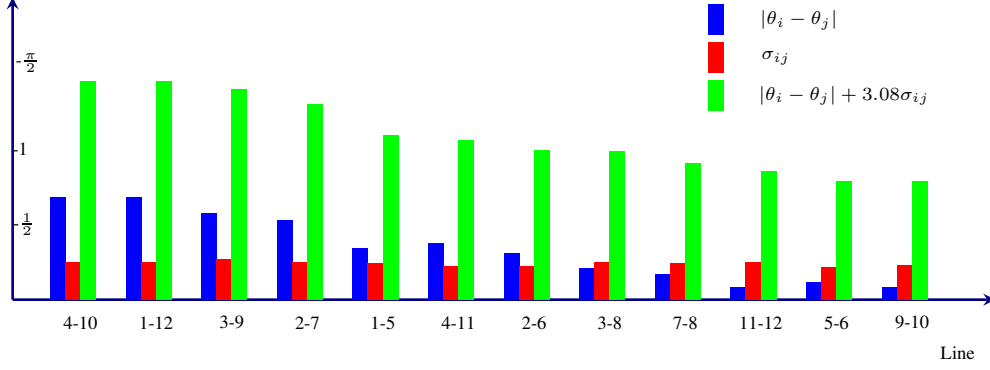


Figure 6: The outputs of the ring network starting from [20,18,25]

red-colored nodes with power supply, 1, 2, 3 and 4, and eight blue-colored nodes with power demand. As for the Manhattan-grid network, the inertias and damping coefficients for nodes with power supply are relatively larger than those of power demand nodes. Due to the ring network structure, every neighborhood is connected to only two other neighborhoods, for example, the neighborhood (2, 6, 7) only directly connects to the neighborhoods (1, 5, 12) and (3, 8, 9). The power network is inspired by [60], and the variance of a ring network structure is less than that of a tree-like structure for a rate $(1 - \frac{1}{n})$ when they are subject to the same disturbances [53], where n is the number of nodes of these two network structures. Also, the authors in [34] introduced a method of curing dead ends in power network by formulating a small ring structure. The outcomes for a group of asymmetric network parameters starting from the power supply vector [20,18,25] are plotted in Fig. 6 and exhibited in Table 9 and the outcomes from another initial vector [23,19,24] are presented in Table 10.

Table 11 and Table 12 show the comparison of the performance for several lines of the power system without and with control as described in the introduction of Section 4. The tables show that, for the power line with the highest values of $\kappa_k(p_s)$, there is a significant reduction of the mean value $|\theta_{i_k} - \theta_{j_k}|$ and a small change of the standard deviation σ_{i_k, j_k} , while the probability exiting the safe set of that line decreases a lot. Table 12 displays the tail probabilities computed according to Table 11. Fig. 7 shows the effect of control on the probability density function of a power flow.

The conclusions of this example are:

1. The nonconvexity property of the control objective function has been additionally illustrated in this example. See Tables 9 and 10 for two power supply vectors starting from different initial state.
2. There is a subset of two power lines of which both members have approximately the same values for the variable $|\theta_{i_k} - \theta_{j_k}| + r \sigma_{i_k, j_k}$. See Fig. 6.
3. In case the parameter values correspond to a symmetric network, then the power lines which connect neighborhoods, $5-6 > 7-8 > 9-10 > 11-12$ in Fig. 5, have little power flow. The fluctuations of the power flows on those lines are not so high. For parameter values of an asymmetric network, there are relatively small power flows in those power lines. See the length of the blue bars of these lines in Fig. 6, the sum of the absolute value of the phase-angle differences plus a multiplier of their standard deviation can not be neglected at all. Therefore, it is always necessary to consider the mean and the standard deviation of the power flow together.

Table 9: Example 4.4. The minimum value and optimal power vector starting from the power supply vector [20,18,25].

Minimum	p_1	p_2	p_3	p_4	p_5	p_6
1.4455	21.7314	19.3050	23.0071	19.9564	-6	-10
	p_7	p_8	p_9	p_{10}	p_{11}	p_{12}
	-8	-12	-17	-13	-7	-11

Table 10: Example 4.4. The minimum and optimal power vector starting from the power supply vector [23,19,24].

Minimum	p_1	p_2	p_3	p_4	p_5	p_6
1.4455	21.6905	19.2546	23.0549	20.0000	-6	-10
	p_7	p_8	p_9	p_{10}	p_{11}	p_{12}
	-8	-12	-17	-13	-7	-11

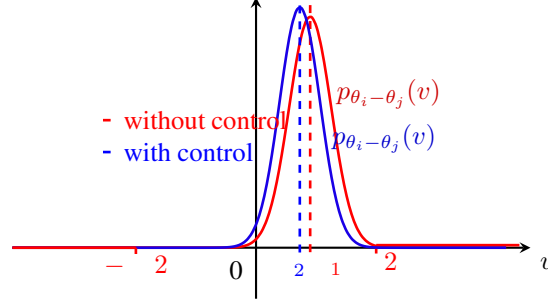


Figure 7: Example. Ring network, line 1-12, without and with control.

Table 11: Example 4.4 The ring network. Comparison of performance without and with control.

Nodes		Control	$ i_k - j_k $	θ_k	$ i_k - j_k + r_\epsilon \theta_k$
i_k	k				
1	12	without	0.7074	0.2753	1.5552
1	12	with	0.5720	0.2646	1.3870
4	10	without	0.6902	0.2517	1.4656
4	10	with	0.6747	0.2502	1.4455
3	9	without	0.6602	0.2492	1.4278
3	9	with	0.6755	0.2500	1.4455
2	7	without	0.5534	0.2512	1.3272
2	7	with	0.5213	0.2495	1.2896
11	12	without	0.1927	0.2510	0.9659
11	12	with	0.0831	0.2490	0.8500

Example 4.5 A Manhattan-grid network.

The power network is displayed in Fig. 8. There are four red-colored nodes 1, 2, 3, and 4 with power supply with high inertias and damping coefficients which provide power to 21 blue-colored nodes with power demand with low virtual inertias and low damping coefficients. One may define for each node with only a power source, an imaginary neighborhood of nodes with only power demand which are largely supplied power by that particular power source. Then the power network is partitioned into several such neighborhoods and between such neighborhoods there is little power exchange. The Manhattan-grid power network has such an interpretation. The computation results for the case of parameter values of an asymmetric power network, are shown in Fig. 9.

The reader finds in Table 13 the results for the comparison without and with control and the corresponding exit probability from the safe set in Table 14. Here we can see the exit probability from the safe set of the most vulnerable line $1-7$ does not decrease as much as line $1-12$ of the ring network. That's because due to the network structure, the power grid is already very stable.

The conclusions of this example are:

Table 12: The exit probabilities of the ring network according to Table 11, both without control and with control. See the notations in Remark 4.3.

Power line	Without control probabilities		With control probabilities		$P_{out,k}$
	a,k	b,k	a,k	b,k	
1-12	6.41e-17	8.56e-04	2.79e-16	8.01e-05	$2 \times 1.90e-04$
4-10	1.32e-19	2.34e-04	11.42e-19	1.71e-04	$2 \times 1.71e-04$
3-9	1.74e-19	1.29e-04	1.29e-19	1.71e-04	$2 \times 1.71e-04$
2-7	1.38e-17	2.56e-05	2.53e-17	1.30e-05	$2 \times 1.70e-04$
11-12	2.00e-08	1.06e-12	1.15e-09	1.55e-11	$2 \times 1.70e-04$

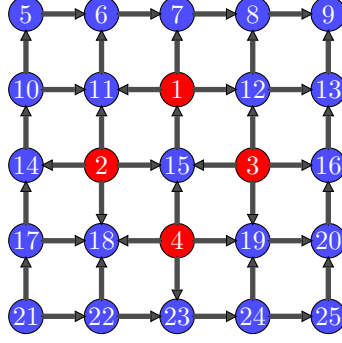


Figure 8: A Manhattan-grid like network

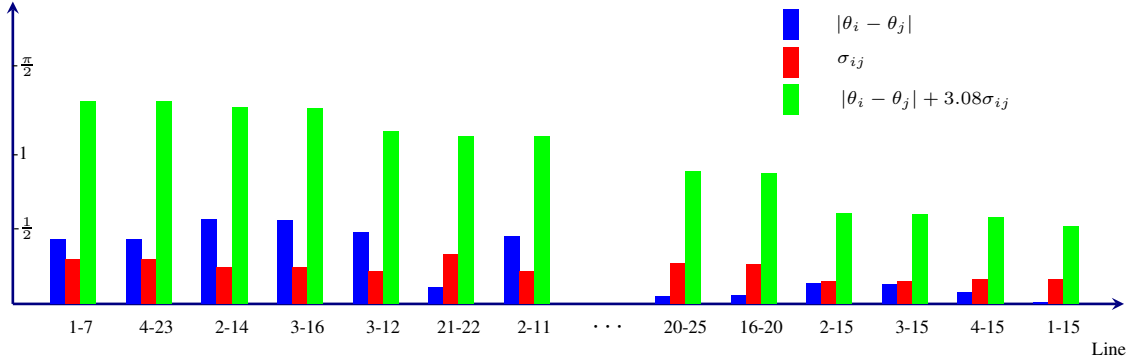


Figure 9: The outputs of the Manhattan-grid like network

1. For this particular example the values of the standard deviations $\sigma_{i,j}$ are relatively high compared with those of $|i - j|$.
2. The reader may observe that for this particular power system, the power flowing from a node with power supply is larger than the power flow of any power line connected to that node, and, similarly, for the nodes with power demand. But no power outage is likely to occur, due to the tight interconnections of the Manhattan power grid, see Fig. 9. Thus, this particular power network has a very stable dynamic behavior due to the grid structure and the large number of power lines.
3. The optimization algorithm used is better than a method based on a grid of the feasible set of power supply vectors. This conclusion has been verified by a computation based on a grid of power supply vectors and by computation of the control objective function at each grid point. The minimal values of the second method are in general larger than those of our proposed algorithm while the computation time is also larger.
4. A starting point for a vector of power supplies for our proposed algorithm may be taken as the sum of all nodes with power demands in a neighborhood of each node with power supply. The computational efficiency can be improved by such an initial choice.

4.1 Conclusions of All Three Examples

1. The descending order of the magnitude of the values of $k(p_s)$ of power lines of a stochastic power system, differ significantly from those of a deterministic power system, Figs. 4, 6, 9, where the columns are ordered in the descending order for the variable $k(p_s) = |i_k - j_k| + r_\epsilon \sigma_{(i_k, j_k)}$. The orders are different in case of the values of the absolute mean $|i_k - j_k|$ and of the standard deviation $\sigma_{(i_k, j_k)}$.
2. A byproduct of the computations is that it is directly clear which power lines have to be monitored by the power system operators during the short horizon for an exit from the safe set. For example, the first four power lines with the highest values in Fig. 9, are best monitored.

Table 13: Example 4.5. The Manhattan-grid network. Comparison of performance without and with control.

Nodes		Control	$i_k - j_k$	θ_k	$i_k - j_k + r_\epsilon \theta_k$
k	k				
1	7	without	0.5363	0.3149	1.5062
1	7	with	0.4990	0.3128	1.4625
4	23	without	0.5363	0.3128	1.4997
4	23	with	0.5046	0.3110	1.4625
3	16	without	0.5574	0.2589	1.3550
3	16	with	0.5932	0.2601	1.3943
2	14	without	0.5574	0.2590	1.3550
2	14	with	0.5932	0.2600	1.3941

Table 14: The exit probabilities of the Manhattan-grid network according to Table 13, both without control and with control. See the notations in Remark 4.3.

Power line	Without control probabilities		With control probabilities		
	a,k	b,k	a,k	b,k	$P_{out,k}$
1-7	1.11e-11	5.10e-04	1.83e-11	3.06e-04	2×3.06e-04
4-23	8.13e-12	4.71e-04	1.25e-11	3.04e-04	2×3.04e-04
3-16	1.02e-16	4.53e-05	4.40e-17	8.55e-05	2×2.36e-04
2-14	1.04e-16	4.56e-05	4.29e-17	8.50e-05	2×2.36e-04

3. The reader sees from the length of the bars $k(p_s) = |i - j| + r_\epsilon \theta_{ij}$, Figs. 4, 6, 9, that there is a subset of power lines of which all members have approximately the same values. This phenomenon is a property of the optimal solution for the considered examples.
4. The Manhattan grid network is much stable than the ring network, due to its network structure.
5. In general, the proposed procedure is better than a computation method based on gridding the feasible set of power supply vectors into equal lengths in terms of efficiency, while their accuracies are comparable.
6. The Braess paradox also occurs in a stochastic power system.
7. The power line with the highest exit probability from the safe subset without control is reduced in probability. Because the power supply has to equal power demand, the control input has the effect that several power lines with exit probabilities below the value of ϵ , will with control have a higher probability of exiting than without control, though all values are still below the threshold of ϵ . See line $3-9$ in Table 12, and line $3-16$, line $2-14$ in Table 14. This issue is due to the choice of the control objective function.
8. The control objective function values of the local minimizers computed by the proposed procedure approach each other, and therefore, one can determine the economic power injection among this set of safe options.

5 Conclusions and Further Research

The emphasis of this paper on control of the phase-angle differences of power lines of a power system, is regarded as a useful focus for control of power systems. The power flows through all power lines of the power network are the main characteristics of a power system as a network. The concept of a safe set and the probability that the phase-angle difference of any power line will exit the safe set, are useful concepts for the control of a stochastic power system. The results for the three examples show clearly that the performance as measured by the sum of the mean value and of a multiple of the standard deviation, differs from that of only the mean value or of only the standard deviation.

Needed for control theory of power systems and of stochastic system is further research on how the performance of the power system depends on: the graph of the power network and the distribution over the nodes of the power supplies and of the standard deviations of the disturbances. In addition, further research is needed on the performance of a power system with very low inertia in all nodes. Moreover, as mentioned in the literature review, this research may be extended to the framework of the Security-Constrained Optimal Power Flow methodology. Especially in a probabilistic way, where the economic cost on power dispatch can also be investigated.

References

References

- [1] S. Abhyankar, G. Geng, M. Anitescu, X. Wang, and V. Dinavahi. Solution techniques for transient stability-constrained optimal power flow – part i. *IET Generation, Transmission & Distribution*, 11(12):3177–3185, 2017.
- [2] P. Alejandro, R. Claudio, A. Enrique, and M. Jose. Directional derivative-based transient stability-constrained optimal power flow. *IEEE Transactions on Power Systems*, 32(5):3415–3426, 2017.
- [3] A. Arapostathis, S. Sastry, and P. Varaiya. Global analysis of swing dynamics. *IEEE Transactions on Circuits and Systems*, 29(10):673–679, 1982.
- [4] J. Baillieul and C. Byrnes. Geometric critical point analysis of lossless power system models. *IEEE Transactions on Circuits and Systems*, 29(11):724–737, 1982.
- [5] M. M. Bhaskar, M. Srinivas, and S. Maheswarapu. Security constraint optimal power flow(scopf)- a comprehensive survey. *Global Journal of Technology and Optimization*, 2(11), 2011.
- [6] H.-D. Chiang, M. W. Hirsch, and F. F. Wu. Stability regions of nonlinear autonomous dynamical systems. *IEEE Transactions on Automatic Control*, 33(1):16–27, 1988.
- [7] E. Davison. Connectability and structural controllability of composite systems. *Automatica*, 13:109–123, 1977.
- [8] Z. Y. Dong, J. H. Zhao, and D. J. Hill. Numerical simulation for stochastic transient stability assessment. *IEEE Transactions on Power Systems*, 27(4):1741–1749, 2012.
- [9] F. Dörfler and F. Bullo. Synchronization and transient stability in power networks and nonuniform Kuramoto oscillators. *SIAM Journal on Control and Optimization*, 50(3):1616–1642, 2012.
- [10] F. Dörfler, M. Chertkov, and F. Bullo. Synchronization in complex oscillator networks and smart grids. *Proceedings of the National Academy of Sciences*, 110(6):2005–2010, 2013.
- [11] F. Dörfler and S. Grammatico. Gather-and-broadcast frequency control in power systems. *Automatica*, 79:296 – 305, 2017.
- [12] F. Dörfler, J. W. Simpson-Porco, and F. Bullo. Breaking the hierarchy: distributed control and economic optimality in microgrids. *IEEE Transactions on Control of Network Systems*, 3(3):241–253, 2016.
- [13] M. Fazlyab, F. Dörfler, and V. M. Preciado. Optimal network design for synchronization of coupled oscillators. *Automatica*, 84:181–189, 2017.
- [14] M. Frank. The braess paradox. *Mathematical Programming*, 20(1):283–302, 1981.
- [15] I. Gikhman and A. Skorokhod. *Introduction to the theory of random processes*. W.B. Saunders Co., Philadelphia, 1969.
- [16] K. Glover and L. Silverman. Characterization of structural controllability. *IEEE Transactions on Automatic Control*, 21:534–537, 1976.
- [17] V. J. Gutierrez-Martinez, C. A. Cañizares, C. R. Fuente-Esquivel, A. Pizano-Martinez, and X. Gu. Neural-network security-boundary constrained optimal power flow. *IEEE Transactions on Power Systems*, 26(1):63–72, 2010.
- [18] H. Haehne, K. Schmietendorf, S. Tamrakar, J. Peinke, and S. Kettelman. Propagation of wind-power induced fluctuations in power grids. *Physical Review E*, 99:050301, 2019.
- [19] R. Hasminski. *Stochastic stability of differential equations*. Sijthoff & Noordhoff, Alphen aan de Rijn, 1980.
- [20] M. D. Ilić and J. Zaborszky. *Dynamics and control of large electric power systems*. Wiley New York, 2000.
- [21] S. Jafarpour, E. Y. Huang, K. D. Smith, and F. Bullo. Flow and elastic networks on the n -torus: Geometry, analysis, and computation. *SIAM Review*, 64(1):59–104, 2022.
- [22] S. Jafarpour, E. Y. Huang, K. D. Smith, and F. Bullo. Flow and elastic networks on the n -torus: Geometry, analysis, and computation. *SIAM Review*, 64(1):59–104, 2022.
- [23] S. C. Johnson, J. D. Rhodes, and M. E. Webber. Understanding the impact of non-synchronous wind and solar generation on grid stability and identifying mitigation pathways. *Applied Energy*, 262:114492, 2020.
- [24] I. Karatzas and S. Shreve. *Brownian motion and stochastic calculus*. Springer-Verlag, Berlin, 1988.
- [25] F. Kozin. A survey of stability of stochastic systems. *Automatica J.-IFAC*, 5:95–112, 1969.
- [26] P. Kundur. *Power system stability and control*. McGraw-Hill, New York, 1994.

- [27] P. Kundur, J. Paserba, V. Ajjarapu, G. Andersson, A. Bose, C. Canizares, N. Hazziargyriou, D. Hill, A. Stankovic, T. van Cutsem, and V. Vittal. Definition and classification of power system stability. *IEEE Transactions on Power Systems*, 19:1387–1401, 2004.
- [28] H. Kunita. Supports of diffusion processes and controllability problems. In *Proceedings International Symposium on Stochastic Differential Equations, Kyoto 1976*, pages 163–185, 1976.
- [29] H. Kushner. *Stochastic stability and control*. Academic Press, New York, 1967.
- [30] H. Kwakernaak and R. Sivan. *Linear optimal control systems*. Wiley-Interscience, New York, 1972.
- [31] C. Li, Y. Liu, and M. R. Gardner. Transient stability analysis with phase plane of high-order derivatives of angle dynamics. In *2014 IEEE PES T&D Conference and Exposition*, pages 1–5. IEEE, 2014.
- [32] N. Li, C. Zhao, and L. Chen. Connecting automatic generation control and economic dispatch from an optimization view. *IEEE Transactions on Control of Network Systems*, 3(3):254–263, 2016.
- [33] E. Marris. Upgrading the grid: Electricity grids must cope with rising demand and complexity in a changing world. emma marris explores the intricacies involved in controlling the power supply. *Nature*, 454(7204):570–574, 2008.
- [34] P. J. Menck, J. Heitzig, J. Kurths, and H. Joachim Schellnhuber. How dead ends undermine power grid stability. *Nature communications*, 5(1):3969, 2014.
- [35] S. Meyn and R. Tweedie. *Markov chains and stochastic stability*. Springer, New York, 1993.
- [36] J. Mohammadi, G. Hug, and S. Kar. Agent-based distributed security constrained optimal power flow. *IEEE Transactions on Smart Grid*, 9(2):1118–1130, 2016.
- [37] A. Monticelli, M. V. F. Pereira, and S. Granville. Security-constrained optimal power flow with post-contingency corrective rescheduling. *IEEE Transactions on Power Systems*, 2(1):175–180, 1987.
- [38] A. E. Motter, S. A. Myers, M. Anghel, and T. Nishikawa. Spontaneous synchrony in power-grid networks. *Nature Physics*, 9(3):191–197, 2013.
- [39] K. Murota. *Matrices and matroids for systems analysis*. Springer-Verlag, Berlin, 2000.
- [40] N. Nguyen, S. Almasabi, A. Bera, and J. Mitra. Optimal power flow incorporating frequency security constraint. *IEEE Transactions on Industry Applications*, 55(6):6508–6516, 2019.
- [41] M. Perninge, V. Knazkins, M. Amelin, and L. Soder. Risk estimation of critical time to voltage instability induced by saddle-node bifurcation. *IEEE Transactions on Power Systems*, 25(3):1600–1610, 2010.
- [42] B. K. Poolla, S. Bolognani, and F. Dörfler. Optimal placement of virtual inertia in power grids. *IEEE Transactions on Automatic Control*, 62(12):6209–6220, 2017.
- [43] S. J. Skar. Stability of multi-machine power systems with nontrivial transfer conductances. *SIAM Journal on Applied Mathematics*, 39(3):475–491, 1980.
- [44] S. Smulders. Control of freeway traffic flow by variable speed signs. *Transportation Research Part B: Methodological*, 24(2):111–132, 1990.
- [45] Y. Song, D. J. Hill, and T. Liu. Network-based analysis of small-disturbance angle stability of power systems. *IEEE Transactions on Control of Network Systems*, 5(3):901–912, 2017.
- [46] R. Steinberg and W. I. Zangwill. The prevalence of Braess’ paradox. *Transportation Science*, 17(3):301–318, 1983.
- [47] E. Tegling, B. Bamieh, and D. F. Gayme. The price of synchrony: Evaluating the resistive losses in synchronizing power networks. *IEEE Transactions on Control of Network Systems*, 2(3):254–266, Sept 2015.
- [48] J. J. Thomas and S. Grijalva. Flexible security-constrained optimal power flow. *IEEE Transactions on Power Systems*, 30(3):1195–1202, 2015.
- [49] H. Trentelman, A. Stoorvogel, and M. Hautus. *Control theory for linear systems*. Springer, United Kingdom, 2001.
- [50] N. Tsolas, A. Arapostathis, and P. Varaiya. A structure preserving energy function for power system transient stability analysis. *IEEE Transactions on Circuits and Systems*, 32(10):1041–1049, 1985.
- [51] M. Vrakopoulou, M. Katsampani, K. Margellos, J. Lygeros, and G. Andersson. Probabilistic security-constrained ac optimal power flow. In *2013 IEEE Grenoble Conference*, pages 1–6. IEEE, 2013.
- [52] J. Walrand and P. P. Varaiya. *High-performance communication networks*. Morgan Kaufmann, 2000.

- [53] Z. Wang, K. Xi, A. Cheng, H. X. Lin, A. C. Ran, J. H. van Schuppen, and C. Zhang. Synchronization of power systems under stochastic disturbances. *Automatica*, 151:110884, 2023.
- [54] Z. Wang, K. Xi, A. Cheng, H. X. Lin, and J. H. van Schuppen. Control of the power flows of a stochastic power system. Report arxiv.2311.16282v1, eess.SY, arXiv, 27 Nov. 2023.
- [55] Z. Wang, K. Xi, A. Cheng, H. X. Lin, and J. H. van Schuppen. Optimal control of a stochastic power system – algorithms and mathematical analysis. Report arXiv.2401.16879, math.OE, 30 Jan. 2024.
- [56] D. Witthaut and M. Timme. Braess’s paradox in oscillator networks, desynchronization and power outage. *New Journal of Physics*, 14(8):083036, aug 2012.
- [57] X. Wu, K. Xi, A. Cheng, H. C. Lin, and J. H. van Schuppen. Increasing the synchronization stability in complex networks. *Chaos*, 33:043116, 2023.
- [58] X. Wu, K. Xi, A. Cheng, C. Zhang, and H. X. Lin. A critical escape probability formulation for enhancing the stability of power systems with system parameter design. Report arxiv.2309.06803v1, arXiv, 13 September 2023.
- [59] K. Xi, J. L. Dubbeldam, H. X. Lin, and J. H. van Schuppen. Power-imbalance allocation control of power systems-secondary frequency control. *Automatica*, 92:72–85, 2018.
- [60] K. Xi, J. L. A. Dubbeldam, and H. X. Lin. Synchronization of cyclic power grids: equilibria and stability of the synchronous state. *Chaos*, 27(1):013109, 2017.
- [61] J. Zaborszky, G. Huang, T. Leung, and B. Zheng. Stability monitoring on the large electric power system. In *Proc. 24th Conference on Decision and Control*, pages 787–798, New York, 1985. IEEE Press.
- [62] J. Zaborszky, G. Huang, B. Zheng, and T. C. Leung. On the phase portrait of a class of large nonlinear dynamic systems such as the power system. *IEEE Transactions on Automatic Control*, 33(1):4–15, Jan 1988.
- [63] J. Zaborszky, K. Whang, K. Prasad, and I. Katz. Local feedback stabilization of large interconnected power system in emergencies. *Automatica*, 17:673–686, 1981.

Zhen Wang was born in China, September 1995. He received his bachelor diploma in computational mathematics from Ningxia University, Yinchuan, China, in 2017. During 2015–2016, he attended the School of Mathematics of Jilin University. He has received in June 2024 a Ph.D. degree from the School of Mathematics of Shandong University, in Jinan, Shandong Province, China. From November 2021 till February 2024, he has been a visiting Ph.D. student at the Department of Applied Mathematics of Delft University of Technology in Delft, The Netherlands.

His research interests include computational mathematics, control theory, optimization, and stability analysis of power systems.

Kaihua Xi was awarded a Ph.D. degree by the Delft Institute of Applied Mathematics, Delft University of Technology, Delft, The Netherlands, in 2018. Currently, he is an associate professor at the School of Mathematics of Shandong University, Jinan, Shandong University, China.

His research interests include control, optimization and stability analysis of power systems, numerical algorithms of differential equations, and data assimilation of oil reservoir simulation.

Aijie Cheng is Full Professor at the School of Mathematics, Shandong University, in Jinan, Shandong Province, China.

His research interests include numerical approximation of partial differential equations, and computational problems of science and engineering.

Hai Xiang Lin received a Ph.D. degree from Delft University of Technology. He is an associate professor at the Department of Mathematical Physics, Delft Institute of Applied Mathematics, Delft University of Technology. He is also a professor in Data Analytics for Environmental Modelling at the Institute of Environmental Sciences of Leiden University, on behalf of the R. Timman Foundation.

His research interests include high-performance computing, atmospheric and environmental modelling, data assimilation, big data, machine learning, simulation, and control of power systems. He has published more than 150 peer-reviewed Journal and international conference papers.

Dr. Lin is an Associate Editor of the journal *Algorithms and Computational Technology*, and an editorial board member of *Big Data Mining and Analytics*.

J. H. van Schuppen (Life Member, IEEE). Jan H. van Schuppen was born in Veenendaal, The Netherlands, October 1947. He was awarded an engineering diploma by Delft University of Technology in 1970 and a Ph.D. diploma in Electrical Engineering and Computer Science by the University of California at Berkeley, CA, USA in 1973.

As Professor Emeritus he is affiliated with the Department of Applied Mathematics of Delft University of Technology in Delft, The Netherlands since his retirement in October 2012 from the Centre of Mathematics and Computer Science (CWI). Since then he is active as a researcher with his consulting company Van Schuppen Control Research in Amsterdam, The Netherlands. His research interests include stochastic control and control of power systems.

Van Schuppen is a member of the IEEE Societies of Control Systems, Computers, and Information Theory, and of the Society for Industrial and Applied Mathematics (SIAM). He was an Associate-Editor-at-large of the *IEEE Transactions on Automatic Control*, a co-editor-in-Chief of the journal *Mathematics of Control, Signals, and Systems*, and was a Department Editor of *J. of Discrete-Event Dynamic Systems*.

The following appendices are included in the paper only for the review process. If the paper is accepted for publication then these appendices will be removed from the paper unless the Editor-in-Chief or the Associate Editor requests differently.

.1 Theory and Proofs of Section 2

.1.1 The Laplacian Matrix for a Complete Power Network

A complete network is defined as a network where every pair of distinct vertices is connected by a unique edge. In this case, the product $B - F(s)$ in equation (9) satisfies,

$$\begin{aligned} (B - F(s))_{i,j} &= -\cos(\theta_{s,i} - \theta_{s,j}) \\ &\quad \forall (i,j) \in \mathcal{E} \text{ with } i \neq j; \\ (B - F(s))_{k,k} &= -\sum_{j=1, j \neq k}^{n_V} (B - F(s))_{k,j} \quad \forall k \in \mathcal{E} \end{aligned}$$

.1.2 Standard Deviation Strictly Positive

Proposition .1 (a) Consider the deterministic linear system from an input u to an output y ,

$$\begin{aligned} \dot{x}(t) &= J(s) x(t) + K u(t) \quad x(0) = x_0 \\ y(t) &= C x(t) \end{aligned}$$

Recall Assumption 2.2. Assume that the diagonal matrix K has strictly positive diagonal elements, hence, for all $k \in \mathcal{V}$, $K_{k,k} < 0$. A weaker condition is that (J_r, K_r) is a controllable pair. Then this system is a controllable system.

(b) For any power line $(i,j) \in \mathcal{E}$ and any fixed power supply vector $p_s \in \mathbb{R}^+$, the standard deviation $\sigma_k(p_s)$ is strictly positive, $\sigma_k(p_s) = (\sigma_{y,(k,k)})^{1/2} < 0$.

Proof (a) (a.1) Consider the following Lyapunov equation for the variance of the phase-angle differences over the power lines,

$$\begin{aligned} 0 &= J(s) \Sigma_x + \Sigma_x J(s)^\top + K K^\top \\ \Sigma_y &= C \Sigma_x C^\top \\ J(s) &= \begin{bmatrix} 0 & & & \\ & -1 & & \\ & & B - F(s) & \\ & & & -1 \end{bmatrix} \begin{bmatrix} I_{n_V} \\ & & & -1 \end{bmatrix} D \end{aligned}$$

Because the Laplacian matrix $B - F(s)$ has one zero eigenvalue, it is required to carry out a transformation and to truncate the system matrix $J(s)$ to eliminate the zero eigenvalue, as described in [53]. Denote the combined transformation and truncation matrix as follows and then note the transformation of the Lyapunov equation,

$$\begin{aligned} n_{x_r} &= n_x - 1 \in \mathbb{R}^{n_{x_r} \times n_{x_r}} \\ J_r &= J(s)^\top K_r = K_r C_r = C_r^\top \\ \Sigma_{x_r} &= \Sigma_x^\top; \\ 0 &= J_r \Sigma_{x_r} + \Sigma_{x_r} J_r^\top + K_r K_r^\top; \quad \text{spec}(J_r) \subset \mathbb{C}^-; \\ \Sigma_y &= C_r \Sigma_{x_r} C_r^\top = C_r^\top \Sigma_{x_r} C_r^\top = C_r \Sigma_{x_r} C_r^\top \end{aligned}$$

(a.2) It will be argued that the tuple $(J_r > K_r)$ is a controllable pair.

Define the undirected state graph $G_X = (X > E_X)$ with node set $X = \mathbb{Z}_{n_x}$ and edge set E_X by $(i > j) \in E_X$ if $J(i > 0)_{i,j} \neq 0$. Recall that $n_x = 2n_y$. Define the input-to-state graph as the undirected graph $G_{UX} = (UX > E_{UX})$ with $UX = \mathbb{Z}_{n_y} \times \mathbb{Z}_{n_y}$ and $(i > j) \in E_{UX}$ if $K_{i,k} \neq 0$.

Recall 2.2, that the graph of the power network is a connected set. It then follows from this assumption that, for any tuple $(i > j) \in E_X$, there exists a path from i to j .

Recall from the assumption of part (a) that for all $i \in \mathbb{Z}_{n_y}$, $K_{k,k} < 0$. It then follows that, for any $i + n_y \in \mathbb{Z}_{n_x}$, there exists a $j \in \mathbb{Z}_{n_y}$ and a path from u_k to i . Because the differential equation of the power system includes the equation that, for all $i \in \mathbb{Z}_{n_y}$, $\dot{i}(t) = -i(t)$, there exists for each such i an integer $m \in \mathbb{Z}_{n_y}$ and a path from u_k to i via $i + n_y = i$.

(a.3) From Theorem [39, Thm. 6.4.2] follows that the time-invariant linear system is controllable if and only if (1) there exists a set of mutually disjoint cycles and stems such that all nodes of X are covered; and (2) for every node of a state there exists a path from an input to that state. This is also proven in [16]. That condition (1) holds follows from the assumption that the power network is a connected set. It was proven above that condition (2) holds. Thus the tuple $(J(i > 0) > K)$ is a controllable pair. The same conclusion holds for the tuple $(J_r > K_r)$ because the deletion of a component with a zero eigenvalue for all concerned matrices does not affect the controllability property, except that it now applies to the truncated linear system.

(b) It follows from $\text{spec}(J_r) \subset \mathbb{C}^-$, $(J_r > K_r)$ a controllable pair, and [49, Thm. 3.28] for the direction that (1) and (2) imply (3), that $\bullet_{x_r} > 0$, hence is strictly positive-definite and symmetric. Recall the notation, $C(i)$ represent the i -th row of the matrix C , the first part of which equals the i -th column of the incidence matrix B . It then follows from the definition of the matrix B that there are two nonzero elements of $C(i)$. This result and $\bullet_{x_r} > 0$ imply that, $\mathfrak{J}_k = (\bullet_{y,(k,k)})^{1/2} = (C(i) \bullet_{x_r} C(i)^T)^{1/2} < 0 > \forall i \in \mathbb{Z}_{n_\varepsilon}$

.1.3 Formulas of $A_1 > 1 > 2$ of Def. 2.5

$$\begin{aligned} \bullet > &\in \mathbb{Z}_{n^+ - 1} > 1 > 2 \in \mathbb{R}^{n^+ - 1} > \\ 1(\bullet) &= p_{sum}^- - p_{n^+}^{+,max} - \dots - p_{i+1}^{+,max} > 2(\bullet) = p_i^{+,max} > \\ A_1(\bullet >) &= \begin{cases} 1 & \text{if } \bullet \leq \\ 0 & \text{if } \bullet < \end{cases} > A_1 \in \mathbb{R}^{(n^+ - 1) \times (n^+ - 1)} \end{aligned}$$

.1.4 Proof of Proposition 2.12

Proof (a) Denote respectively the probability density function and the probability distribution function of $G(0 > 1)$ by $p_G : \mathbb{R} \rightarrow \mathbb{R}_+$ and $G : \mathbb{R} \rightarrow \mathbb{R}_+$. Because p_G is symmetric when mirrored at 0, thus for all $v \in \mathbb{R}$, $p_G(v) = p_G(-v)$, it follows that, for all $r \in \mathbb{R}$, $1 - G(r) = G(-r)$.

For all $i \in \mathbb{Z}_{n_\varepsilon}$, and for all $p_s \in \mathbb{R}^+$, the probability that the power flow of the i -th power line goes into the unstable region according to the invariant probability distribution of the power line flow, is equal to,

$$\begin{aligned} &p_{out,k}(p_s) \\ &= (\{ \omega \in \Omega \mid i_k(\omega) - j_k(\omega) < -2 \}) + \\ &+ (\{ \omega \in \Omega \mid i_k(\omega) - j_k(\omega) < +2 \}) \\ &= \left(\left\{ \omega \in \Omega \mid \frac{(\theta_{i_k}(\omega,t) - \theta_{j_k}(\omega,t)) - m_k(p_s)}{\sigma_k(p_s)} \right. \right. \\ &\quad \left. \left. < \frac{-\pi/2 - m_k(p_s)}{\sigma_k(p_s)} \right\} \right) + \\ &= G_{(0,1)}(r_{a,k}(p_s)) + [1 - G_{(0,1)}(r_{b,k}(p_s))] \\ &= G_{(0,1)}(r_{a,k}(p_s)) + G_{(0,1)}(-r_{b,k}(p_s)) > \\ r_{a,k}(p_s) &= \frac{2 - k(p_s)}{\mathfrak{J}_k(p_s)} > \end{aligned}$$

$$\begin{aligned}
-r_{b,k}(p_s) &= \frac{-2 + \angle_k(p_s)}{\angle_k(p_s)} > \\
r_{a,b,k}(p_s) &= \frac{-2 + |\angle_k(p_s)|}{\angle_k(p_s)} > \\
\angle_k(p_s) \in (-2 > + 2) &\Rightarrow \\
r_{a,k}(p_s) < 0 > -r_{b,k}(p_s) < 0
\end{aligned}$$

Because the probability distribution function G is strictly monotone, the definition of $r_{a,b,k}$ and the monotonicity of G imply the inequality of $G(r_{a,b,k}(p_s))$.

(b) By definition $G_{(0,1)}(r_{\epsilon/2}) \leq 2$, for example, if $2 = 10^{-3}$ then $r_{\epsilon/2} = -3.08$. Assume that $r_{a,b,k}(p_s) \leq r_{\epsilon/2}$. Then,

$$\begin{aligned}
r_{a,k}(p_s) &\leq \max\{r_{a,k}(p_s) > -r_{b,k}(p_s)\} \\
&= r_{a,b,k}(p_s) \leq r_{\epsilon/2} > \text{and similarly,} \\
-r_{b,k}(p_s) &\leq \max\{r_{a,k}(p_s) > -r_{b,k}(p_s)\} \\
&= r_{a,b,k}(p_s) \leq r_{\epsilon/2} > \Rightarrow \\
p_{out,k}(p_s) &= G_{(0,1)}(r_{a,k}(p_s)) + G_{(0,1)}(-r_{b,k}(p_s)) \\
&\leq
\end{aligned}$$

The existence of $p_s^* \in \mathbb{R}^+$ follows from a result of [55] and the lower bound from the implications,

$$\begin{aligned}
\angle_k^* < 2 &\Rightarrow \forall \epsilon \in \mathbb{Z}_{n_\epsilon} > \\
r_{a,b,k}(p_s^*) &= \frac{-2 + |\angle_k(p_s^*)|}{\angle_k(p_s^*)} \leq \frac{-2 + \angle_k^*}{\angle_k^*} + r_\epsilon \leq r_\epsilon \\
p_{out,k}(p_s^*) &\leq 2
\end{aligned} \tag{17}$$

Note that if $\angle_k^* < 2$, let $\frac{-\pi/2 + \angle_k^*}{\sigma_k(p_s^*)} + r_\epsilon = r_{\epsilon_{new}}$, then it satisfies that $r_{\epsilon_{new}} < r_\epsilon$. We can further get that $p_{out,k}(p_s^*) \leq 2_{new}$. Furthermore, in the first inequality of (17), the '=' is satisfied if and only if line is the most vulnerable line according to our criterion.

2 Theory of Section 3

2.1 Computation of the matrices A and Λ of $r_{a,s,k}(p_s)$ in Def. 3.1

By Theorem 2.3 and [13, Prop. 1], the sin values of phase-angle differences satisfy $\sin(B^\top \theta) = B^\top (B B^\top)^\dagger p_{sp}$ and then we transform the matrix $(B B^\top)^\dagger$ into a diagonal matrix: $\hat{\Lambda}^\top (B B^\top)^\dagger \hat{\Lambda} = \Lambda \Rightarrow (B B^\top)^\dagger = \hat{\Lambda}^\dagger \hat{\Lambda}^\top$. Define $\hat{\Lambda} = \hat{\Lambda}^\top$, which makes $(B B^\top)^\dagger = \hat{\Lambda}^\dagger \Lambda^\dagger$. Recall the notation that $\hat{\Lambda}_i$ represents the i -th column of the matrix $\hat{\Lambda}$. Define $p_s \in \mathbb{R}^{(n^+-1) \times 1}$, $p_d \in \mathbb{R}^{(n^v-n^+) \times 1}$, $A \in \mathcal{R}^{n_\epsilon \times (n^+-1)} \in \mathcal{R}^{n_\epsilon \times 1}$ by the following formulas:

$$\begin{aligned}
p_s &= [p_1 > p_2 > \cdots > p_{n^+-1}]^\top > \\
-p_d &= [-p_{n^++1} > -p_{n^++2} > \cdots > -p_n]^\top ; \\
&= B^\top \hat{\Lambda}^\dagger \Lambda^\dagger [\hat{\Lambda}_1 - \hat{\Lambda}_{n^+} > \cdots > \hat{\Lambda}_{n^+-1} - \hat{\Lambda}_{n^+}] p_s + \\
&\quad + B^\top \hat{\Lambda}^\dagger \Lambda^\dagger [\hat{\Lambda}_{n^++1} - \hat{\Lambda}_{n^+} > \cdots > \hat{\Lambda}_n - \hat{\Lambda}_{n^+}] p_d \\
A &= B^\top \hat{\Lambda}^\dagger \Lambda^\dagger [\hat{\Lambda}_1 - \hat{\Lambda}_{n^+} > \cdots > \hat{\Lambda}_{n^+-1} - \hat{\Lambda}_{n^+}] > \\
&= B^\top \hat{\Lambda}^\dagger \Lambda^\dagger [\hat{\Lambda}_{n^++1} - \hat{\Lambda}_{n^+} > \cdots > \hat{\Lambda}_n - \hat{\Lambda}_{n^+}] p_d ;
\end{aligned}$$

then, it follows that,

$$\begin{aligned}
B^\top (B B^\top)^\dagger p_{sp} &= B^\top \Lambda^\dagger p_{sp} \\
&= B^\top \Lambda^\dagger \begin{bmatrix} p_1 & \dots & p_{n+1} & p_{sum}^- - p_1 - \dots - p_{n+1} \\ -p_{n+1}^{-,max} & \dots & -p_n^{-,max} \end{bmatrix}^\top \\
&= B^\top \Lambda^\dagger (p_1 (1 - \alpha_{n+1}) + \dots + p_{n+1} (\alpha_{n+1} - \alpha_n) \\
&\quad + p_{sum}^- - p_{n+1}^{-,max} - \dots - p_n^{-,max}) \\
&= B^\top \Lambda^\dagger (p_1 (1 - \alpha_{n+1}) + \dots + p_{n+1} (\alpha_{n+1} - \alpha_n) \\
&\quad + p_{n+1}^{-,max} (\alpha_n - \alpha_{n+1}) + \dots + p_n^{-,max} (\alpha_n - \alpha_n)) \\
&= A p_s +
\end{aligned} \tag{18}$$

Supplement of 'Control of the Power Flows of a Stochastic Power System'

Zhen Wang *

July 16, 2024

1 Introduction

The purpose for this supplement is to provide the direct outcomes of the proposed procedure for the three examples investigated in the main body of the paper. The parameters of specific power systems can be used for computations and are listed so as to allow reproduction. From these results, the readers may learn the proposed procedure. Furthermore, the figures in the manuscript are plotted based on the particular tables listed in this supplement. Fig. 4 is based on Table 5; Fig. 6 is based on Table 36; and Fig. 9 is based on Table 47.

Paper organization Section 2 deals with the particular eight-node academic example. Its original parameters and original outcomes are listed. Afterward, some of the parameters of this particular power network or the network structure are changed in order to investigate their influence on the outcomes.

Section 3 deals with a twelve-node ring network, its network structure is symmetric, we first make every kind of parameter symmetric to investigate the outcomes. Secondly, every kind of parameter is changed in order to see its influence on the outcomes.

Section 4 deals with a Manhattan-grid network. Since it is a symmetric network structure, we first make every kind of parameter symmetric to see what will the outcomes look like. Next, we make the power demand vector asymmetric and similarly the disturbance vector, to compare the results. Since this network is large, it will cost more time to compute the minimizer than small networks, hence we do not investigate the influence on the outcomes by changing the network parameters of this power system. Additionally, Sections 3 and 4 also compare the computation results of a power system with and without applying the proposed procedure.

*Zhen Wang is with the School of Mathematics, Shandong University, Jinan, 250100, Shandong Province, China, and visited the Dept. of Applied Mathematics, Delft University of Technology, Delft, The Netherlands from November 2021 to February 2024 (email: wangzhen17@mail.sdu.edu.cn, wangzhen17.sdu@vip.163.com). Zhen Wang is grateful to the China Scholarship Council (No. 202106220104) for financial support for his stay at Delft University of Technology in Delft, The Netherlands.

2 Tables of the Particular Eight-Node Academic Example

The picture of the particular eight-node academic network is displayed in Fig. 1 where the nodes 1, 2, 3, 4 have only power supply and the other nodes have only power demand. Tables 1 and 2 show the network parameters of this particular eight-node academic power system, to make these parameters realistic, the inertias and the damping coefficients of the power supply nodes are set to be larger than those of the power demand nodes. Table 3 displays the maximum power supply and the predicted power demand of each node, one can check that these specified values indeed satisfy our Definition 2.3 in the main body of the paper.

Table 4 shows the minimum of the control objective function and the optimal power supply vector computed by our proposed procedure. Table 5 shows the absolute value of mean of the phase-angle difference of each power line: $|\theta_i - \theta_j|$, the standard deviation of the phase-angle difference σ_{ij} , the component of our object function $|\theta_i - \theta_j| + 3.08 \sigma_{ij}$ and the power flow $l_{ij} \sin(|\theta_i - \theta_j| + 3.08 \sigma_{ij})$ of each power line and the rows of this table are sorted by $|\theta_i - \theta_j| + 3.08 \sigma_{ij}$ in a descending order. What's more, this computation result is by applying the initial point [12, 14, 13]. In this example, the parameter r_ϵ is chosen as 3.08, which leads to the probability that the phase-angle differences of all power lines exceed the safety subset is less than 0.2%. As comparison groups, the other two results are computed by our procedure through the initial point [12, 12, 12], [11, 11, 14], separately and the results are displayed in Tables 6 and 7 and Tables 8 and 9. With the comparisons, the nonconvexity of the control objective function has been verified, which means that starting from different initial points, one can find different local minimizers. The computation has been additionally evaluated by discretizing the domain of the power supply vectors for each dimension into a grid with 150 steps. The minimum value computed by this grid method is 1.3529 which is smaller or equal than the values computed by our proposed procedure from these three initial points. The results of this gridding method are shown in Tables 10 and 11.

By increasing the strength or intensity of the disturbances to 1.2 times before, the computational results are shown in Tables 12, 13, Tables 14, 15, and Tables 16, 17, starting from [12, 14, 13], [12, 12, 12], [11, 11, 14] separately. From these tables, one can see the values of the minima have increased and are closer to $\pi/2$ now. Additionally, one can see the minimizers in Table 12 and Table 15 differ a little while the minimizer in Table 17 differs a lot with these two vectors of minimizers.

Tables 22 and 23 show the outcomes after adding line 2 – 4 while Tables 18 and 19 present the consequences after doubling the capacity of line 3 – 4. The results of the comparison groups of these two cases are shown in Tables 24, 25, and Tables 20, 21, separately. After adding a new line or doubling the capacity of one line, one expects the power system to become more stable than before, but in fact it becomes worse. See the comparisons of Table 22 with Table 5 and Table 18 with Table 5.

Furthermore, readers can also conclude that the minimum values are very close to each other even if the minimizers differ obviously from these tables. Moreover, the largest value and second largest value of vector $|\theta_i - \theta_j| + 3.08 \sigma$ differ very little and this may be due to the optimal solution. Last but not least, the control objective is to maintain the phase-angle differences over power lines inside the safety region, and a comparison should be made of the stochastic power system without and with using the proposed procedure. Here, we use the *proportional control law* as the form of without using the proposed procedure, and the comparison results are shown in Table 26, followed by the tail probability computed by this table. Here, with the tail probability we mean the probability of the power flow going outside the safety region. Note that the tail probability of line $i - j$ computed by our control objective function is two times an upper bound of the largest value of $P(\omega \in \Omega \mid \theta_{ij}(\omega, t) < -\pi/2)$ and $P(\omega \in \Omega \mid \theta_{ij}(\omega, t) > \pi/2)$, and these two probabilities are computed according to the real expectations of the phase-angle differences. Some of them are positive while the rest of them are negative. From Table 26, we can see the probabilities of the two vulnerable lines going out of the safety region drop down tremendously, while this tail probability of the other lines may increase. This is because of the choice of our control objective function, what we want to adjust is the most vulnerable line while the other lines may be less stable than before, see line 6-7, line 2-7, line 1-7 etc.

Finally, we provide evidence that the power system is more stable after using our proposed procedure than without using the procedure in a practical sense, by increasing the power demand to approach the maximal available power supply. This is a contingency that happens a lot in practice when large consumer centers like steel factories or data centers change the value of their power demand due to a change in activities, and the same for steel factories. We still assume the maximal power supply is larger than the sum of power demand, otherwise, there is a need for load shedding. We set the sum of power demand is 59 which almost reaches the maximal power supply 60. The computation results are shown in Tables 28, 29, 30.

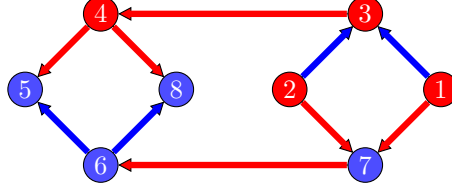


Figure 1: The particular eight-node academic example

Table 1: The network parameters:

$i,$	Node	1	2	3	4	5	6	7	8
$m_i,$	Inertia	10	10	10	10	1	1	1	1
$d_i,$	Damping	4	4	4	4	1	1	1	1
$K_2(i, i),$	Disturbance	1.7668	1.9482	1.5724	1.4638	2.2385	2.4133	2.1685	2.2157

Table 2: Line capacities

Line	1-3	1-7	2-3	2-7	3-4	4-5	4-8	5-6	6-7	6-8	2-4
Capacities	25	25	25	25	25 or 50	25	25	25	25	25	0 or 25

Table 3: Power supply and power demand

Power	$p_1^{+,max}$	$p_2^{+,max}$	$p_3^{+,max}$	$p_4^{+,max}$	$p_5^{-,max}$	$p_6^{-,max}$	$p_7^{-,max}$	$p_8^{-,max}$
	12	14	16	18	12	12	13	13

Table 4: The minimum and optimal power vector start from the power supply vector [12, 12, 12]

Minimum	p_1	p_2	p_3	p_4	p_5	p_6	p_7	p_8
1.3530	11.7679	13.7632	13.5247	10.9441	-12	-12	-13	-13

Table 5: Phase-angle differences and other outputs start from the power supply vector [12, 12, 12]

i	j	$ \theta_i - \theta_j $	σ_{ij}	$ \theta_i - \theta_j + 3.08\sigma_{ij}$	$l_{ij} \sin(\theta_i - \theta_j + 3.08\sigma_{ij})$
6	7	0.5274	0.2681	1.3530	24.4096
4	8	0.5217	0.2699	1.3529	24.4089
4	5	0.4988	0.2694	1.3284	24.2692
2	7	0.5605	0.2239	1.2500	23.7248
1	7	0.5140	0.2230	1.2007	23.3076
3	4	0.5695	0.1648	1.0770	22.0132
6	8	0.0216	0.2658	0.8402	18.6193
5	6	0.0016	0.2659	0.8205	18.2871
2	3	0.0189	0.1267	0.4091	9.9452
1	3	0.0210	0.1247	0.4051	9.8535
				$1.57 \approx \pi/2$	

Table 6: The minimum and optimal power vector start from the power supply vector [12, 14, 13]

Minimum	p_1	p_2	p_3	p_4	p_5	p_6	p_7	p_8
1.3529	11.8411	13.8306	13.3145	11.0138	-12	-12	-13	-13

Table 7: Phase-angle differences and other outputs start from the power supply vector [12, 14, 13]

i	j	$ \theta_i - \theta_j $	σ_{ij}	$ \theta_i - \theta_j + 3.08\sigma_{ij}$	$l_{ij}\sin(\theta_i - \theta_j + 3.08\sigma_{ij})$
6	7	0.5273	0.2681	1.3529	24.4090
4	8	0.5217	0.2699	1.3529	24.4089
4	5	0.4988	0.2693	1.3284	24.2692
2	7	0.5604	0.2239	1.2499	23.7239
1	7	0.5141	0.2229	1.2007	23.3075
3	4	0.5660	0.1646	1.0730	21.9663
6	8	0.0216	0.2658	0.8402	18.6186
5	6	0.0016	0.2659	0.8205	18.2864
2	3	0.0217	0.1267	0.4121	10.0126
1	3	0.0181	0.1248	0.4023	9.7891

Table 8: The minimum and optimal power vector start from the power supply vector [11, 11, 14]

Minimum	p_1	p_2	p_3	p_4	p_5	p_6	p_7	p_8
1.3532	11.7085	12.6649	15.2572	10.3694	-12	-12	-13	-13

Table 9: Phase-angle differences and other outputs start from the power supply vector [11, 11, 14]

i	j	$ \theta_i - \theta_j $	σ_{ij}	$ \theta_i - \theta_j + 3.08\sigma_{ij}$	$l_{ij}\sin(\theta_i - \theta_j + 3.08\sigma_{ij})$
4	8	0.5218	0.2700	1.3532	24.4107
6	7	0.5273	0.2682	1.3532	24.4106
4	5	0.4988	0.2694	1.3287	24.2711
2	7	0.5482	0.2238	1.2375	23.6240
1	7	0.5259	0.2231	1.2130	23.4168
3	4	0.5969	0.1657	1.1071	22.3606
6	8	0.0216	0.2658	0.8402	18.6191
5	6	0.0016	0.2659	0.8205	18.2869
1	3	0.0337	0.1245	0.4172	10.1289
2	3	0.0146	0.1263	0.4036	9.8180

Table 10: The minimum and optimal power vector by gridding method

Minimum	p_1	p_2	p_3	p_4	p_5	p_6	p_7	p_8
1.3529	11.9329	13.9333	13.0203	11.1135	-12	-12	-13	-13

Table 11: Phase-angle differences and other outputs by gridding method

i	j	$ \theta_i - \theta_j $	σ_{ij}	$ \theta_i - \theta_j + 3.08\sigma_{ij}$	$l_{ij}\sin(\theta_i - \theta_j + 3.08\sigma_{ij})$
4	8	0.5218	0.2698	1.3529	24.4088
6	7	0.5273	0.2680	1.3528	24.4085
4	5	0.4988	0.2693	1.3284	24.2691
2	7	0.5605	0.2239	1.2500	23.7246
1	7	0.5139	0.2229	1.2005	23.3059
3	4	0.5613	0.1645	1.0679	21.9044
6	8	0.0216	0.2658	0.8401	18.6183
5	6	0.0016	0.2659	0.8204	18.2861
2	3	0.0257	0.1268	0.4163	10.1085
1	3	0.0143	0.1248	0.3987	9.7051

Table 12: Increase the strength of the disturbance to 1.2 times before, the minimum value and optimal power vector start from the power supply vector [12, 12, 12]

Minimum	p_1	p_2	p_3	p_4	p_5	p_6	p_7	p_8
1.5188	11.8169	13.7957	13.4565	10.9308	-12	-12	-13	-13

Table 13: Increase the strength of the disturbance to be 1.2 times before, phase-angle differences and other output start from the power supply vector [12, 12, 12]

i	j	$ \theta_i - \theta_j $	σ_{ij}	$ \theta_i - \theta_j + 3.08\sigma_{ij}$	$l_{ij} \sin(\theta_i - \theta_j + 3.08\sigma_{ij})$
4	8	0.5214	0.3238	1.5188	24.9663
6	7	0.5279	0.3217	1.5188	24.9662
4	5	0.4985	0.3232	1.4940	24.9264
2	7	0.5606	0.2687	1.3881	24.5838
1	7	0.5145	0.2676	1.3386	24.3289
3	4	0.5693	0.1977	1.1782	23.0978
6	8	0.0219	0.3189	1.0041	21.0925
5	6	0.0019	0.3190	0.9845	20.8249
2	3	0.0202	0.1520	0.4884	11.7313
1	3	0.0194	0.1497	0.4804	11.5535

Table 14: Increase the strength of the disturbance to be 1.2 times before, the minimum value and optimal power vector start from the power supply vector [12, 14, 13]

Minimum	p_1	p_2	p_3	p_4	p_5	p_6	p_7	p_8
1.5188	11.8003	13.7608	13.5348	10.9041	-12	-12	-13	-13

Table 15: Increase the strength of the disturbance to be 1.2 times before, phase-angle differences and other output start from the power supply vector [12, 14, 13]

i	j	$ \theta_i - \theta_j $	σ_{ij}	$ \theta_i - \theta_j + 3.08\sigma_{ij}$	$l_{ij} \sin(\theta_i - \theta_j + 3.08\sigma_{ij})$
6	7	0.5280	0.3217	1.5188	24.9663
4	8	0.5214	0.3238	1.5188	24.9663
4	5	0.4985	0.3232	1.4940	24.9264
2	7	0.5604	0.2687	1.3879	24.5829
1	7	0.5147	0.2676	1.3388	24.3302
3	4	0.5705	0.1978	1.1796	23.1113
6	8	0.0219	0.3189	1.0041	21.0926
5	6	0.0019	0.3190	0.9845	20.8250
2	3	0.0189	0.1520	0.4872	11.7030
1	3	0.0203	0.1497	0.4812	11.5715

Table 16: Increase the strength of the disturbance to be 1.2 times before, the minimum value and optimal power vector start from the power supply vector [11, 11, 14]

Minimum	p_1	p_2	p_3	p_4	p_5	p_6	p_7	p_8
1.5192	11.7376	12.7167	15.1915	10.3543	-12	-12	-13	-13

Table 17: Increase the strength of the disturbance to be 1.2 times before, phase-angle differences and other output start from the power supply vector [11, 11, 14]

i	j	$ \theta_i - \theta_j $	σ_{ij}	$ \theta_i - \theta_j + 3.08\sigma_{ij}$	$l_{ij}\sin(\theta_i - \theta_j + 3.08\sigma_{ij})$
6	7	0.5279	0.3218	1.5192	24.9667
4	8	0.5214	0.3239	1.5192	24.9667
4	5	0.4985	0.3233	1.4943	24.9270
2	7	0.5488	0.2686	1.3760	24.5272
1	7	0.5260	0.2677	1.3505	24.3960
3	4	0.5969	0.1988	1.2093	23.3842
6	8	0.0219	0.3189	1.0042	21.0931
5	6	0.0019	0.3191	0.9845	20.8255
1	3	0.0326	0.1494	0.4927	11.8257
2	3	0.0130	0.1516	0.4798	11.5408

Table 18: Doubling capacity of line 3 – 4, the minimum and optimal power vector start from the power supply vector [12, 12, 12]

Minimum	p_1	p_2	p_3	p_4	p_5	p_6	p_7	p_8
1.3712	12.0001	14.0000	16.0000	7.9999	-12	-12	-13	-13

Table 19: Doubling capacity of line 3 – 4, the phase-angle differences and other outputs start from the power supply vector [12, 12, 12]

i	j	$ \theta_i - \theta_j $	σ_{ij}	$ \theta_i - \theta_j + 3.08\sigma_{ij}$	$l_{ij}\sin(\theta_i - \theta_j + 3.08\sigma_{ij})$
4	8	0.5552	0.2649	1.3712	24.5037
4	5	0.5319	0.2644	1.3463	24.3728
6	7	0.4620	0.2600	1.2628	23.8239
2	7	0.5269	0.2198	1.2040	23.3372
1	7	0.4812	0.2186	1.1544	22.8638
5	6	0.0271	0.2651	0.8435	18.6750
6	8	0.0071	0.2650	0.8233	18.3348
3	4	0.3652	0.1371	0.7875	35.4282
2	3	0.0572	0.1418	0.4939	11.8509
1	3	0.0171	0.1377	0.4412	10.6757

Table 20: Doubling the capacity of line 3 – 4, the minimum value and optimal power vector start from the power supply vector [12, 14, 13]

Minimum	p_1	p_2	p_3	p_4	p_5	p_6	p_7	p_8
1.3712	12.0001	14.0000	16.0000	7.9999	-12	-12	-13	-13

Table 21: Doubling the capacity of line 3 – 4, the phase-angle differences and other outputs start from the power supply vector [12, 14, 13]

i	j	$ \theta_i - \theta_j $	σ_{ij}	$ \theta_i - \theta_j + 3.08\sigma_{ij}$	$l_{ij}\sin(\theta_i - \theta_j + 3.08\sigma_{ij})$
4	8	0.5552	0.2649	1.3712	24.5037
4	5	0.5319	0.2644	1.3463	24.3728
6	7	0.4620	0.2600	1.2628	23.8239
2	7	0.5269	0.2198	1.2040	23.3372
1	7	0.4812	0.2186	1.1544	22.8638
5	6	0.0271	0.2651	0.8435	18.6750
6	8	0.0071	0.2650	0.8233	18.3348
3	4	0.3652	0.1371	0.7875	35.4283
2	3	0.0572	0.1418	0.4939	11.8510
1	3	0.0171	0.1377	0.4412	10.6758

Table 22: Adding line 2 – 4, the minimum value and optimal power vector start from the power supply vector [12, 12, 12]

Minimum	p_1	p_2	p_3	p_4	p_5	p_6	p_7	p_8
1.3953	12.0000	14.0000	16.0000	7.9999	-12	-12	-13	-13

Table 23: Adding line 2 – 4, the phase-angle differences and other outputs start from the power supply vector [12, 12, 12]

i	j	$ \theta_i - \theta_j $	σ_{ij}	$ \theta_i - \theta_j + 3.08\sigma_{ij}$	$l_{ij} \sin(\theta_i - \theta_j + 3.08\sigma_{ij})$
4	8	0.5670	0.2689	1.3953	24.6161
4	5	0.5435	0.2683	1.3700	24.4975
1	7	0.5536	0.2236	1.2424	23.6636
6	7	0.4398	0.2584	1.2356	23.6089
2	7	0.4334	0.2197	1.1101	22.3934
3	4	0.4588	0.1444	0.9036	19.6386
5	6	0.0372	0.2649	0.8529	18.8299
6	8	0.0171	0.2648	0.8326	18.4926
2	4	0.2957	0.1356	0.7135	16.3612
2	3	0.1520	0.1055	0.4770	11.4789
1	3	0.0457	0.1293	0.4439	10.7365

Table 24: Adding line 2 – 4, the minimum value and optimal power vector start from the power supply vector [12, 14, 13]

Minimum	p_1	p_2	p_3	p_4	p_5	p_6	p_7	p_8
1.3953	12.0001	14.0000	16.0000	7.9999	-12	-12	-13	-13

Table 25: Adding line 2 – 4, the phase-angle differences and other outputs start from the power supply vector [12, 14, 13]

i	j	$ \theta_i - \theta_j $	σ_{ij}	$ \theta_i - \theta_j + 3.08\sigma_{ij}$	$l_{ij} \sin(\theta_i - \theta_j + 3.08\sigma_{ij})$
4	8	0.5670	0.2689	1.3953	24.6161
4	5	0.5435	0.2683	1.3700	24.4975
1	7	0.5536	0.2236	1.2424	23.6636
6	7	0.4398	0.2584	1.2356	23.6089
2	7	0.4334	0.2197	1.1101	22.3934
3	4	0.4588	0.1444	0.9036	19.6386
5	6	0.0372	0.2649	0.8529	18.8299
6	8	0.0171	0.2648	0.8326	18.4925
2	4	0.2957	0.1356	0.7135	16.3612
2	3	0.1520	0.1055	0.4770	11.4789
1	3	0.0457	0.1293	0.4439	10.7365

Table 26: Phase-angle differences and other outputs for particular eight-node network without and with applying the procedure, the initial power supply vector is [12, 12, 12]

Procedure	i	j	$ \theta_i - \theta_j $	σ_{ij}	$ \theta_i - \theta_j + 3.08 \sigma_{ij}$	$l_{ij} \sin(\theta_i - \theta_j + 3.08 \sigma_{ij})$
without	4	8	0.5566	0.2711	1.3917	24.5999
with	4	8	0.5217	0.2699	1.3529	24.4089
without	4	5	0.5332	0.2705	1.3664	24.4796
with	4	5	0.4988	0.2694	1.3284	24.2692
without	6	7	0.4593	0.2647	1.2747	23.9121
with	6	7	0.5274	0.2681	1.3530	24.4096
without	2	7	0.5217	0.2219	1.2051	23.3472
with	2	7	0.5605	0.2239	1.2500	23.7248
without	1	7	0.4836	0.2210	1.1644	22.9642
with	1	7	0.5140	0.2230	1.2007	23.3076
without	3	4	0.4519	0.1605	0.9463	20.2809
with	3	4	0.5695	0.1648	1.0770	22.0132
without	5	6	0.0283	0.2658	0.8470	18.7324
with	5	6	0.0016	0.2659	0.8205	18.2871
without	6	8	0.0083	0.2657	0.8267	18.3919
with	6	8	0.0216	0.2658	0.8402	18.6193
without	1	3	0.0650	0.1258	0.4525	10.9301
with	1	3	0.0210	0.1247	0.4051	9.8535
without	2	3	0.0317	0.1278	0.4253	10.3137
with	2	3	0.0189	0.1267	0.4091	9.9452

Table 27: Tail Probability of the particular Eight-node network according to Table 26

Procudure	i	j	$P(\omega \in \Omega \theta_{ij}(\omega, t) < -\pi/2)$	$P(\omega \in \Omega \theta_{ij}(\omega, t) > \pi/2)$	by our criterion (Upper bound)
without	4	8	2.1259e-15	9.1630e-05	
with	4	8	4.4924e-15	5.0749e-05	$2 \times 5.0755e - 05$
without	4	5	3.6789e-15	6.2566e-05	
with	4	5	7.8163e-15	3.4574e-05	$2 \times 5.0443e - 05$
without	6	7	1.3400e-05	8.6386e-15	
with	6	7	4.9748e-05	2.5148e-15	$2 \times 4.9635e - 05$
without	2	7	2.0523e-21	1.1349e-06	
with	2	7	8.7456e-22	3.2069e-06	$2 \times 2.5311e - 05$
without	1	7	7.2975e-21	4.3396e-07	
with	1	7	4.4298e-21	1.0739e-06	$2 \times 2.4889e - 05$
without	3	4	1.0232e-36	1.5699e-12	
with	3	4	7.2278e-39	6.1675e-10	$2 \times 5.3733e - 06$
without	5	6	8.9299e-10	3.2526e-09	
with	5	6	1.8016e-09	1.6747e-09	$2 \times 4.8277e - 05$
without	6	8	2.0429e-09	1.3979e-09	
with	6	8	1.0431e-09	2.7976e-09	$2 \times 4.8216e - 05$
without	1	3	2.5587e-33	5.8703e-39	
with	1	3	9.1864e-36	1.2856e-37	$2 \times 6.9455e - 07$
without	2	3	1.0556e-33	2.2809e-36	
with	2	3	2.0661e-36	8.5471e-35	$2 \times 7.9733e - 07$

Table 28: Increase the power demand to 59, the minimum value and optimal power vector start from the power supply vector is [5, 5, 5]

Minimum	p_1	p_2	p_3	p_4	p_5	p_6	p_7	p_8
1.5306	12.0001	14.001	16.0000	16.9998	-16	-13	-14	-16

Table 29: Increase the power demand to 59, without and with applying the procedure, the initial power supply vector is [5, 5, 5]

Procedure	i	j	$ \theta_i - \theta_j $	σ_{ij}	$\frac{ \theta_i - \theta_j + 3.08 \sigma_{ij}}{3.08 \sigma_{ij}}$	$l_{ij} \sin(\theta_i - \theta_j + 3.08 \sigma_{ij})$
without	4	5	0.6746	0.2801	1.5373	24.9860
with	4	5	0.6687	0.2798	1.5306	24.9798
without	4	8	0.6746	0.2796	1.5358	24.9847
with	4	8	0.6687	0.2793	1.5291	24.9783
without	6	7	0.5834	0.2727	1.4234	24.7290
with	6	7	0.5944	0.2734	1.4366	24.7751
without	2	7	0.6127	0.2272	1.3126	24.1712
with	2	7	0.6187	0.2276	1.3198	24.2166
without	1	7	0.5654	0.2263	1.2623	23.8196
with	1	7	0.5704	0.2266	1.2685	23.8663
without	3	4	0.5718	0.1662	1.0838	22.0939
with	3	4	0.5944	0.1672	1.1093	22.3848
without	5	6	0.0154	0.2694	0.8450	18.6998
with	5	6	0.0200	0.2694	0.8496	18.7759
without	6	8	0.0154	0.2690	0.8441	18.6841
with	6	8	0.0200	0.2691	0.8487	18.7603
without	1	3	0.0638	0.1269	0.4548	10.9811
with	1	3	0.0600	0.1267	0.4502	10.8785
without	2	3	0.0244	0.1289	0.4214	10.2253
with	2	3	0.0200	0.1286	0.4161	10.1048

Table 30: Tail Probability of the particular Eight-node network according to Table 29

Procudure	i	j	$P(\omega \in \Omega \theta_{ij}(\omega, t) < -\pi/2)$	$P(\omega \in \Omega \theta_{ij}(\omega, t) > \pi/2)$	by our criterion (Upper bound)
without	4	5	5.4441e-16	6.8819e-04	
with	4	5	6.0261e-16	6.3190e-04	$2 \times 6.3282e - 04$
without	4	8	4.8441e-16	6.7466e-04	
with	4	8	5.3633e-16	6.1928e-04	$2 \times 6.3225e - 04$
without	6	7	1.4684e-04	1.4000e-15	
with	6	7	1.7760e-04	1.1922e-15	$2 \times 6.2543e - 04$
without	2	7	3.6113e-22	1.2380e-05	
with	2	7	3.2938e-22	1.4372e-05	$2 \times 5.6376e - 04$
without	1	7	1.8699e-21	4.4406e-06	
with	1	7	1.7066e-21	5.0549e-06	$2 \times 5.6221e - 04$
without	3	4	2.5071e-38	9.2300e-10	
with	3	4	1.1788e-38	2.6149e-09	$2 \times 4.4943e - 04$
without	5	6	3.8808e-09	1.9558e-09	
with	5	6	4.2942e-09	1.7637e-09	$2 \times 6.2067e - 04$
without	6	8	1.8549e-09	3.6878e-09	
with	6	8	1.6946e-09	4.1340e-09	$2 \times 6.2031e - 04$
without	1	3	7.9376e-33	2.8800e-38	
with	1	3	4.4264e-33	3.2638e-38	$2 \times 3.4033e - 04$
without	2	3	1.8450e-33	1.7744e-35	
with	2	3	8.6867e-34	1.8965e-35	$2 \times 3.4620e - 04$

3 Tables of a Ring Network Example

The picture of the twelve-node ring network is displayed in Fig. 2. First, a group of symmetric parameters are shown in 31, which leads to the symmetric outputs in Tables 32 and 33. From the three columns of $|\theta_i - \theta_j|$, σ_{ij} , $|\theta_i - \theta_j| + 3.08\sigma_{ij}$ in Table 33, one can see that several transmission lines have very small almost zero power flows but at the same time their fluctuations are serious. Thus, we have justified our choice of the control objective function, i.e. to consider both the mean value and the standard deviation of the phase-angle difference together.

Secondly, several of the parameters are changed to be asymmetric as shown in Tables 34. The computation results are exhibited in Tables 35 and 36 starting from the power supply vector $[20, 28, 15]$ and in Tables 37 and 38 starting from the power supply vector $[23, 19, 24]$. From these four tables, one can see that the lines which connect two neighbourhoods have now small power flows. What's more, the two different initial points lead to slightly different minimizers.

Moreover, as for the particular eight-node academic network, the numerical values for without and with applying our proposed procedure are shown in Table 39. In Table 39, it is observable that the two highest values of $|\theta_i - \theta_j| + 3.08\sigma_{ij}$ have decreased as well. We generate a figure displaying the probability density function of line 1 – 12 for both the 'without applying' and 'with applying' the proposed procedure, as shown in Fig. 3, where the values are borrowed from Table 39. In this depiction, the reduction in both standard deviation and mean value from the 'without applying the proposed procedure to the 'with applying the proposed procedure' is evident. Same as the particular eight-node example, we show the comparison results of applying the proposed procedure and not applying the proposed procedure in Table 39, while the corresponding tail probabilities are shown in Table 40. From Table 40, we can see the tail probability of the most vulnerable line 1 – 12 decreases quite a lot and that of the second vulnerable line decreases a little. What's more, some of the lines may be less stable than before, see line 3 – 9 and line 3 – 8, and the reason of that scenario is due to the choice of the control objective function.

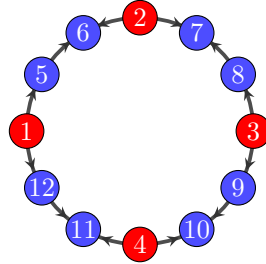


Figure 2: A ring network

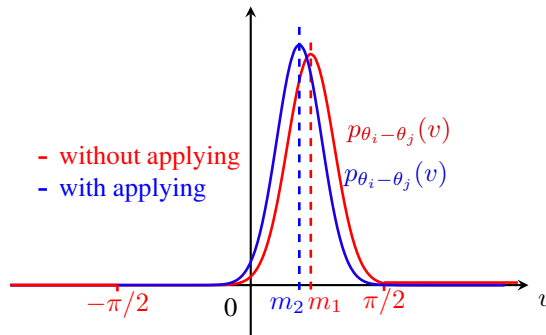


Figure 3: Example. ring network, line 1-12, without and with control.

Table 31: Network parameters, where the line capacities are not shown and they are all equal 20.

Node i	$p^{+,max},$ $-p^{-,max}$	Inertia m_i	Damping d_i	Disturbance $K_2(i, i)$
1	30	10	4	2
2	20	10	4	2
3	25	10	4	2
4	20	10	4	2
5	-10	1	1	2
6	-10	1	1	2
7	-10	1	1	2
8	-10	1	1	2
9	-10	1	1	2
10	-10	1	1	2
11	-10	1	1	2
12	-10	1	1	2

Table 32: The minimum and optimal power vector starting from the power supply vector [20,18,25]

Minimum	p_1	p_2	p_3	p_4	p_5	p_6	p_7	p_8	p_9	p_{10}	p_{11}	p_{12}
1.4221	20.0011	20.0000	19.9989	20.0000	-10	-10	-10	-10	-10	-10	-10	-10

Table 33: Phase-angle differences and other outputs

i	j	$ \theta_i - \theta_j $	σ_{ij}	$ \theta_i - \theta_j + 3.08 \sigma_{ij}$	$l_{ij} \sin(\theta_i - \theta_j + 3.08 \sigma_{ij})$
4	10	0.5236	0.2917	1.4221	19.7792
2	7	0.5236	0.2917	1.4221	19.7792
1	5	0.5236	0.2917	1.4221	19.7792
1	12	0.5236	0.2917	1.4221	19.7792
3	9	0.5236	0.2917	1.4220	19.7789
3	8	0.5236	0.2917	1.4220	19.7789
2	6	0.5236	0.2917	1.4220	19.7789
4	11	0.5236	0.2917	1.4220	19.7789
7	8	2.8213e-05	0.2782	0.8570	15.1180
9	10	2.8205e-05	0.2782	0.8570	15.1180
11	12	2.8217e-05	0.2782	0.8570	15.1180
5	6	2.8208e-05	0.2782	0.8570	15.1180
				$1.57 \approx \pi/2$	

Changing the parameters: Several parameters are changed to be asymmetric.

Table 34: Network parameters, what not listed are that all line capacities are increased to 24

Node i	$p^{+,max},$ $-p^{-,max}$	Inertia m_i	Damping d_i	Disturbance $K_2(i, i)$
1	30	10	4	2.00
2	20	10	4	2.30
3	25	10	4	2.50
4	20	10	4	2.70
5	-6	1	1	1.60
6	-10	1	1	1.70
7	-8	1	1	1.80
8	-12	1	1	1.90
9	-17	1	1	1.65
10	-13	1	1	1.75
11	-7	1	1	1.85
12	-11	1	1	2.05

Table 35: The minimum value and optimal power vector starting from the power supply vector [20,18,25]

Minimum	p_1	p_2	p_3	p_4	p_5	p_6	p_7	p_8	p_9	p_{10}	p_{11}	p_{12}
1.4455	21.7314	19.3050	23.0071	19.9564	-6	-10	-8	-12	-17	-13	-7	-11

Table 36: Phase-angle differences and other outputs

i	j	$ \theta_i - \theta_j $	σ_{ij}	$ \theta_i - \theta_j + 3.08 \sigma_{ij}$	$l_{ij} \sin(\theta_i - \theta_j + 3.08 \sigma_{ij})$
4	10	0.6747	0.2503	1.4455	23.8119
3	9	0.6755	0.2500	1.4455	23.8118
1	12	0.5742	0.2647	1.3896	23.6071
2	7	0.5236	0.2496	1.2923	23.0753
3	8	0.3398	0.2433	1.0891	21.2693
1	5	0.3707	0.2229	1.0573	20.9044
2	6	0.3093	0.2214	0.9913	20.0813
4	11	0.2083	0.2502	0.9790	19.9190
7	8	0.1675	0.2398	0.9060	18.8894
11	12	0.0849	0.2490	0.8519	18.0606
5	6	0.1125	0.2172	0.7814	16.9022
9	10	0.0831	0.2265	0.7807	16.8903

Table 37: The minimum value and optimal power vector starting from the power supply vector [23,19,24]

Minimum	p_1	p_2	p_3	p_4	p_5	p_6	p_7	p_8	p_9	p_{10}	p_{11}	p_{12}
1.4455	21.6905	19.2546	23.0549	20.0000	-6	-10	-8	-12	-17	-13	-7	-11

Table 38: Phase-angle differences and other outputs

i	j	$ \theta_i - \theta_j $	σ_{ij}	$ \theta_i - \theta_j + 3.08 \sigma_{ij}$	$l_{ij} \sin(\theta_i - \theta_j + 3.08 \sigma_{ij})$
3	9	0.6755	0.2500	1.4455	23.8118
4	10	0.6747	0.2502	1.4455	23.8118
1	12	0.5720	0.2646	1.3870	23.5957
2	7	0.5213	0.2495	1.2896	23.0577
3	8	0.3419	0.2433	1.0914	21.2945
1	5	0.3709	0.2229	1.0574	20.9063
2	6	0.3091	0.2214	0.9911	20.0796
4	11	0.2102	0.2502	0.9810	19.9447
7	8	0.1655	0.2398	0.9039	18.8577
11	12	0.0831	0.2490	0.8500	18.0306
5	6	0.1127	0.2172	0.7815	16.9045
9	10	0.0831	0.2265	0.7807	16.8899

Table 39: Phase-angle differences and other outputs for ring network without and with applying the procedure, the initial power supply vector is [23,19,24]

The procedure	i	j	$ \theta_i - \theta_j $	σ_{ij}	$ \theta_i - \theta_j + 3.08 \sigma_{ij}$	$l_{ij} \sin (\theta_i - \theta_j + 3.08 \sigma_{ij})$
without	1	12	0.7074	0.2753	1.5552	23.9971
with	1	12	0.5720	0.2646	1.3870	23.5957
without	4	10	0.6902	0.2517	1.4656	23.8672
with	4	10	0.6747	0.2502	1.4455	23.8118
without	3	9	0.6602	0.2492	1.4278	23.7549
with	3	9	0.6755	0.2500	1.4455	23.8118
without	2	7	0.5534	0.2512	1.3272	23.2917
with	2	7	0.5213	0.2495	1.2896	23.0577
without	1	5	0.4728	0.2268	1.1715	22.1121
with	1	5	0.3709	0.2229	1.0574	20.9063
without	3	8	0.3128	0.2427	1.0602	20.9389
with	3	8	0.3419	0.2433	1.0914	21.2945
without	11	12	0.1927	0.2510	0.9659	19.7410
with	11	12	0.0831	0.2490	0.8500	18.0306
without	7	8	0.1935	0.2405	0.9341	19.2974
with	7	8	0.1655	0.2398	0.9039	18.8577
without	2	6	0.2129	0.2193	0.8882	18.6222
with	2	6	0.3091	0.2214	0.9911	20.0796
without	5	6	0.2069	0.2188	0.8808	18.5096
with	5	6	0.1127	0.2172	0.7815	16.9045
without	4	11	0.1003	0.2502	0.8708	18.3566
with	4	11	0.2102	0.2502	0.9810	19.9447
without	9	10	0.0952	0.2267	0.7934	17.1059
with	9	10	0.0831	0.2265	0.7807	16.8899

Table 40: Tail Probability of the ring network according to Table 39

The procedure	i	j	$P(\omega \in \Omega \theta_{ij}(\omega, t) < -\pi/2)$	$P(\omega \in \Omega \theta_{ij}(\omega, t) > \pi/2)$	by our criterion (Upper bound)
without	1	12	6.4054e-17	8.5576e-04	
with	1	12	2.7878e-16	8.0087e-05	$2 \times 1.9005e - 04$
without	4	10	1.3186e-19	2.3386e-04	
with	4	10	11.4193e-19	1.7080e-04	$2 \times 1.7128e - 04$
without	3	9	1.7355e-19	1.2905e-04	
with	3	9	1.2915e-19	1.7102e-04	$2 \times 1.7102e - 04$
without	2	7	1.3812e-17	2.5593e-05	
with	2	7	2.5329e-17	1.2974e-05	$2 \times 1.7036e - 04$
without	1	5	1.0250e-19	6.4511e-07	
with	1	5	1.5052e-18	3.6604e-08	$2 \times 1.3520e - 04$
without	3	8	4.2129e-15	1.0897e-07	
with	3	8	1.8982e-15	2.1981e-07	$2 \times 1.6220e - 04$
without	11	12	2.0049e-08	1.0636e-12	
with	11	12	1.1527e-09	1.5457e-11	$2 \times 1.6971e - 04$
without	7	8	1.1008e-13	5.1170e-09	
with	7	8	2.2335e-13	2.3104e-09	$2 \times 1.5758e - 04$
without	2	6	2.0838e-16	2.9711e-10	
with	2	6	1.0248e-17	6.0356e-09	$2 \times 1.3321e - 04$
without	5	6	2.2413e-16	2.2802e-10	
with	5	6	4.5620e-15	9.5233e-12	$2 \times 1.2766e - 04$
without	4	11	1.2025e-11	2.0853e-09	
with	4	11	5.4637e-13	2.6936e-08	$2 \times 1.7128e - 04$
without	9	10	3.7820e-11	9.9920e-14	
with	9	10	2.5464e-11	1.4179e-13	$2 \times 1.3997e - 04$

4 Tables of a Manhattan-grid Network Example

The picture of a Manhattan-grid power network with 25 nodes is displayed in Fig. 4 where the nodes 1, 2, 3, 4 provide power supply and the other nodes model power demand. Table 44 shows the parameters of this network. In this example, the symmetric parameters lead to a symmetric optimal power supply vector which is shown in Table 41. Then, we change the power demand vector from a symmetric one to an asymmetric one, which leads to an asymmetric optimal power supply vector in Table 42. What's more, when the vector of disturbance is changed from a symmetric one to an asymmetric one, the power supply also becomes asymmetric, as shown in Table 43.

Tables 45, 46, and 47 show the absolute value of mean of phase-angle difference: $|\theta_i - \theta_j|$, the standard deviation of the phase-angle difference of this power line: σ_{ij} , each component of the control objective vector: $|\theta_i - \theta_j| + 3.08\sigma_{ij}$ and line power flow $l_{ij}\sin(|\theta_i - \theta_j| + 3.08\sigma_{ij})$, and these three tables are ordered by the values of $|\theta_i - \theta_j| + 3.08\sigma_{ij}$ in the descending order. As in the particular eight-node academic network, in contrast with the results in Table 42, the computation has been additionally evaluated by discretizing the set of three power supply vectors for each dimension into a grid with 150 steps and the minimum is 1.3416, which is slightly larger than the value computed by our proposed procedure. Meanwhile, for this power network with large amount of nodes and links, our proposed procedure has a higher efficiency than this partition method.

What's more, from Tables 45, 46, and 47, one can see the total power demand of the neighborhood of a power supply node is much larger than the capacity of the line which connects the neighborhood to this power supply node, e.g. the neighborhood: node 5, 6, 7, 8, 9 and the connection line 1 – 7. If this power network is a tree-like network, then It will experience an immediate power outage. But for this power network, it remains very stable, which is due to its network structure and the number of links.

Furthermore, as for the particular eight-node example, the largest value and the second largest value of the vector $|\theta_i - \theta_j| + 3.08\sigma_{ij}$ differ very little. Moreover, the computations from several different initial power supply vectors are considered, and in each case we have computed, the iteration sequence converged to minimizer which is quite close to each other.

Results of with and without applying the proposed procedure are shown in Tables 48 and 49 for symmetric power demand vector and symmetric disturbance vector. Then we change the strength of disturbance to be asymmetric, the results are shown in Tables 52 and 53. These four tables are ordered by the values of $|\theta_i - \theta_j| + 3.08 * \sigma_{ij}$ in tables of results without applying the proposed procedure. We can see the largest and the second largest values of $|\theta_i - \theta_j| + 3.08 * \sigma_{ij}$ decrease while the other values go up and down. A figure depicting the probability density function for the cases 'without applying' and 'with applying' of line 1 – 7 where the disturbance vectors are asymmetric is presented, as illustrated in Fig. 4. Note that the values are borrowed from in Table 52. In this illustration, the reduction in both standard deviation and mean value from the 'without applying' to the 'with applying' condition is not readily apparent. This is attributed to the small magnitude of the decrease, making it challenging to discern in the visual representation.

Finally, we show the tail probabilities according to Tables 48 and 49 in Tables 50 and 51, and those according to Tables 52 and 53 are shown in Tables 54 and 55. From these tables, one can see the probability of the two most vulnerable lines which go outside the safety region becomes smaller, which means they are more stable than without applying the proposed procedure.

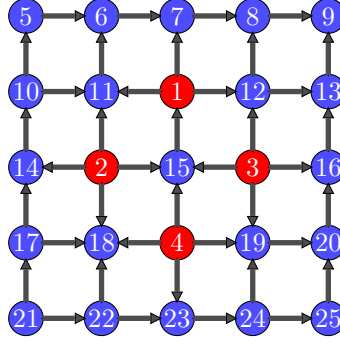


Figure 4: A Manhattan-grid network

Table 41: The minimum value and optimal power vector starting from the power supply vector [45,53,55] for a symmetric power demand vector, and a symmetric disturbance vector

Minimum	p_1	p_2	p_3	p_4	p_5	p_6	p_7	p_8	p_9	p_{10}	p_{11}	p_{12}
1.4253	45.0000	60.0000	60.0000	45.0000	-9.5000	-14	-8	-14	-9.5	-8	-8	-8
p_{13}	p_{14}	p_{15}	p_{16}	p_{17}	p_{18}	p_{19}	p_{20}	p_{21}	p_{22}	p_{23}	p_{24}	p_{25}
-8	-14	-8	-14	-8	-8	-8	-8	-9.5	-14	-8	-14	-9.5

Table 42: The minimum value and optimal power vector starting from the power supply vector [45,53,55] for an asymmetric power demand vector, and a symmetric disturbance vector

Minimum	p_1	p_2	p_3	p_4	p_5	p_6	p_7	p_8	p_9	p_{10}	p_{11}	p_{12}
1.3413	43.1692	60.0000	60.0000	46.8308	-5	-8	-8	-10	-8	-10	-14	-16
p_{13}	p_{14}	p_{15}	p_{16}	p_{17}	p_{18}	p_{19}	p_{20}	p_{21}	p_{22}	p_{23}	p_{24}	p_{25}
-8	-14	-14	-14	-8	-14	-14	-8	-8	-8	-8	-8	-5

Table 43: The minimum value and optimal power vector starting from the power supply vector [45,53,55] for a symmetric power demand vector, and an asymmetric disturbance vector

Minimum	p_1	p_2	p_3	p_4	p_5	p_6	p_7	p_8	p_9	p_{10}	p_{11}	p_{12}
1.4625	44.2792	60.0000	60.0000	45.7208	-9.5000	-14	-8	-14	-9.5000	-8	-8	-8
p_{13}	p_{14}	p_{15}	p_{16}	p_{17}	p_{18}	p_{19}	p_{20}	p_{21}	p_{22}	p_{23}	p_{24}	p_{25}
-8	-14	-8	-14	-8	-8	-8	-8	-9.5000	-14	-8	-14	-9.5000

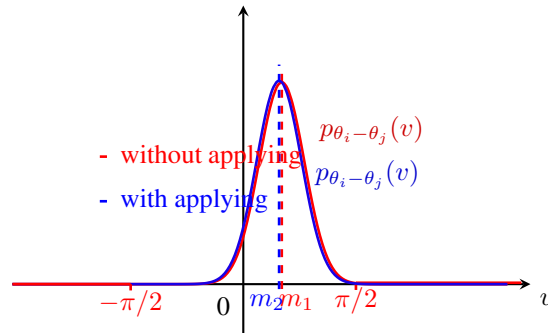


Figure 5: Example. Manhattan-grid network, line 1-7, without and with control, disturbance vector asymmetric.

Table 44: Network parameters in which the line capacity is not listed there, where all line capacities equal 40

Node i	$p^{+,max}$ $-p^{-,max}$ symmetric	$p^{+,max}$ $-p^{-,max}$ asymmetric	Inertia m_i	Damping d_i	Disturbance symmetric $K_2(i, i)$	Disturbance asymmetric $K_2(i, i)$
1	60	60	10	4	2	1.5682
2	60	60	10	4	2	2.0387
3	60	60	10	4	2	1.3929
4	60	60	10	4	2	1.4432
5	-9.5	-5	1	0	2	1.9966
6	-14	-8	1	0	2	2.7663
7	-8	-8	1	0	2	1.6152
8	-14	-10	1	0	2	2.1857
9	-9.5	-8	1	0	2	1.8872
10	-8	-10	1	1	2	2.5587
11	-8	-14	1	1	2	1.4555
12	-8	-16	1	1	2	2.0163
13	-8	-8	1	1	2	2.2763
14	-14	-14	1	1	2	2.5503
15	-8	-14	1	1	2	2.7721
16	-14	-14	1	1	2	2.0430
17	-8	-8	1	1	2	1.2542
18	-8	-14	1	1	2	1.6288
19	-8	-14	1	1	2	1.4692
20	-8	-8	1	1	2	3.1752
21	-9.5	-8	1	0	2	1.6922
22	-14	-8	1	0	2	2.3740
23	-8	-8	1	0	2	1.9038
24	-14	-8	1	0	2	2.4443
25	-9.5	-5	1	0	2	1.6176

Table 45: Phase-angle differences and other outputs, power demand vector symmetric, disturbance vector symmetric

i	j	$ \theta_i - \theta_j $	σ_{ij}	$ \theta_i - \theta_j + 3.08 \sigma_{ij}$	$l_{ij} \sin (\theta_i - \theta_j + 3.08 \sigma_{ij})$
1	7	0.5018	0.2998	1.4253	39.5773
4	23	0.5018	0.2998	1.4253	39.5773
2	14	0.5932	0.2418	1.3379	38.9200
3	16	0.5932	0.2418	1.3379	38.9200
2	18	0.4343	0.2160	1.0997	35.6429
3	19	0.4343	0.2160	1.0997	35.6429
2	11	0.4343	0.2160	1.0997	35.6429
3	12	0.4343	0.2160	1.0997	35.6429
8	9	0.0904	0.3246	1.0900	35.4652
5	6	0.0904	0.3246	1.0900	35.4652
24	25	0.0904	0.3246	1.0900	35.4652
21	22	0.0904	0.3246	1.0900	35.4652
18	22	0.3044	0.2399	1.0434	34.5643
19	24	0.3044	0.2399	1.0434	34.5643
6	11	0.3044	0.2399	1.0434	34.5643
8	12	0.3044	0.2399	1.0434	34.5643
7	8	0.1410	0.2905	1.0358	34.4114
6	7	0.1410	0.2905	1.0358	34.4114
23	24	0.1410	0.2905	1.0358	34.4114
22	23	0.1410	0.2905	1.0358	34.4114
1	12	0.3276	0.2221	1.0116	33.9063
1	11	0.3276	0.2221	1.0116	33.9063
4	19	0.3276	0.2221	1.0116	33.9063
4	18	0.3276	0.2221	1.0116	33.9063
12	13	0.2452	0.2468	1.0055	33.7763
10	11	0.2452	0.2468	1.0055	33.7763
19	20	0.2452	0.2468	1.0055	33.7763
17	18	0.2452	0.2468	1.0055	33.7763
17	21	0.1478	0.2699	0.9792	33.2026
20	25	0.1478	0.2699	0.9792	33.2026
5	10	0.1478	0.2699	0.9792	33.2026
9	13	0.1478	0.2699	0.9792	33.2026
14	17	0.1047	0.2622	0.9123	31.6369
16	20	0.1047	0.2622	0.9123	31.6369
10	14	0.1047	0.2622	0.9123	31.6369
13	16	0.1047	0.2622	0.9123	31.6369
2	15	0.0997	0.1506	0.5635	21.3651
3	15	0.0997	0.1506	0.5635	21.3651
1	15	5.0008e-04	0.1625	0.5010	19.2139
4	15	4.9992e-04	0.1625	0.5010	19.2139
				$1.57 \approx \pi/2$	

Table 46: Phase-angle differences and other outputs, power demand vector asymmetric, disturbance vector symmetric

i	j	$ \theta_i - \theta_j $	σ_{ij}	$ \theta_i - \theta_j + 3.08 \sigma_{ij}$	$l_{ij} \sin(\theta_i - \theta_j + 3.08 \sigma_{ij})$
1	7	0.4285	0.2964	1.3413	38.9515
4	23	0.4285	0.2964	1.3413	38.9515
2	14	0.5614	0.2400	1.3004	38.5470
3	16	0.5547	0.2397	1.2929	38.4649
3	12	0.4742	0.2169	1.1423	36.3841
21	22	0.1100	0.3248	1.1103	35.8330
2	11	0.4453	0.2159	1.1102	35.8319
8	9	0.0910	0.3239	1.0886	35.4392
2	18	0.4155	0.2161	1.0810	35.2966
24	25	0.0722	0.3241	1.0704	35.0949
5	6	0.0703	0.3235	1.0668	35.0266
3	19	0.3984	0.2156	1.0624	34.9418
4	18	0.3529	0.2219	1.0363	34.4201
1	12	0.3477	0.2226	1.0333	34.3590
4	19	0.3410	0.2215	1.0231	34.1494
7	8	0.1334	0.2885	1.0219	34.1242
22	23	0.1203	0.2884	1.0086	33.8443
1	11	0.3154	0.2216	0.9980	33.6155
23	24	0.0957	0.2880	0.9827	33.2808
17	18	0.2110	0.2461	0.9691	32.9745
6	7	0.0826	0.2876	0.9683	32.9573
10	11	0.2046	0.2459	0.9619	32.8115
19	20	0.1971	0.2457	0.9539	32.6265
12	13	0.1907	0.2457	0.9475	32.4785
8	12	0.2094	0.2375	0.9407	32.3197
9	13	0.1094	0.2690	0.9378	32.2493
13	16	0.1199	0.2614	0.9251	31.9470
18	22	0.1910	0.2371	0.9213	31.8551
6	11	0.1889	0.2372	0.9193	31.8082
17	21	0.0903	0.2689	0.9184	31.7852
19	24	0.1775	0.2369	0.9071	31.5079
10	14	0.1018	0.2614	0.9070	31.5063
14	17	0.0808	0.2611	0.8849	30.9547
5	10	0.0548	0.2682	0.8809	30.8526
20	25	0.0529	0.2683	0.8792	30.8086
16	20	0.0571	0.2609	0.8605	30.3279
2	15	0.1337	0.1507	0.5978	22.5138
3	15	0.1291	0.1507	0.5934	22.3657
4	15	0.0753	0.1621	0.5744	21.7340
1	15	0.0128	0.1624	0.5131	19.6341

Table 47: Phase-angle differences and other outputs, power demand vector symmetric, disturbance vector asymmetric

i	j	$ \theta_i - \theta_j $	σ_{ij}	$ \theta_i - \theta_j + 3.08 \sigma_{ij}$	$l_{ij} \sin(\theta_i - \theta_j + 3.08 \sigma_{ij})$
1	7	0.4990	0.3128	1.4625	39.7656
4	23	0.5046	0.3110	1.4625	39.7656
3	16	0.5932	0.2601	1.3943	39.3787
2	14	0.5932	0.2600	1.3941	39.3770
5	6	0.0896	0.3416	1.1416	36.3717
8	9	0.0896	0.3381	1.1310	36.1934
3	12	0.4379	0.2233	1.1255	36.0993
2	11	0.4379	0.2214	1.1199	36.0019
19	24	0.3040	0.2628	1.1135	35.8899
24	25	0.0912	0.3307	1.1099	35.8256
6	11	0.3049	0.2597	1.1046	35.7320
3	19	0.4307	0.2180	1.1022	35.6882
21	22	0.0912	0.3279	1.1012	35.6696
6	7	0.1397	0.3104	1.0959	35.5730
8	12	0.3049	0.2547	1.0895	35.4555
23	24	0.1422	0.3068	1.0870	35.4102
7	8	0.1397	0.3062	1.0829	35.3328
2	18	0.4307	0.2112	1.0812	35.3018
10	11	0.2439	0.2681	1.0695	35.0792
22	23	0.1422	0.3011	1.0695	35.0788
19	20	0.2465	0.2672	1.0694	35.0757
12	13	0.2439	0.2615	1.0495	34.6861
18	22	0.3040	0.2414	1.0475	34.6473
1	12	0.3233	0.2295	1.0302	34.2956
20	25	0.1470	0.2866	1.0297	34.2848
1	11	0.3233	0.2281	1.0259	34.2074
4	19	0.3319	0.2250	1.0250	34.1878
9	13	0.1486	0.2837	1.0224	34.1340
17	18	0.2465	0.2495	1.0149	33.9772
5	10	0.1486	0.2803	1.0119	33.9140
4	18	0.3319	0.2180	1.0033	33.7302
16	20	0.1026	0.2852	0.9809	33.2407
10	14	0.1068	0.2813	0.9731	33.0644
13	16	0.1068	0.2799	0.9689	32.9717
17	21	0.1470	0.2647	0.9621	32.8154
14	17	0.1026	0.2717	0.9396	32.2931
2	15	0.0997	0.1859	0.6723	24.9118
3	15	0.0997	0.1854	0.6706	24.8577
4	15	0.0079	0.1931	0.6025	22.6696
1	15	0.0069	0.1932	0.6018	22.6465

Table 48: Phase-angle differences and other outputs for Manhattan network with and without control, power demand vector symmetric, disturbance vector symmetric

The procedure	i	j	$ \theta_i - \theta_j $	σ_{ij}	$\frac{ \theta_i - \theta_j + 3.08 \sigma_{ij}}{3.08 \sigma_{ij}}$	$\frac{l_{ij} \sin(\theta_i - \theta_j + 3.08 \sigma_{ij})}{3.08 \sigma_{ij}}$
without	1	7	0.5363	0.3017	1.4657	39.7793
with	1	7	0.5018	0.2998	1.4253	39.5773
without	4	23	0.5363	0.3017	1.4657	39.7793
with	4	23	0.5018	0.2998	1.4253	39.5773
without	2	14	0.5574	0.2408	1.2990	38.5317
with	2	14	0.5932	0.2418	1.3379	38.9200
without	3	16	0.5574	0.2408	1.2990	38.5317
with	3	16	0.5932	0.2418	1.3379	38.9200
without	5	6	0.0979	0.3242	1.0963	35.5810
with	5	6	0.0904	0.3246	1.0900	35.4652
without	24	25	0.0979	0.3242	1.0963	35.5810
with	24	25	0.0904	0.3246	1.0900	35.4652
without	8	9	0.0979	0.3242	1.0963	35.5810
with	8	9	0.0904	0.3246	1.0900	35.4652
without	21	22	0.0979	0.3242	1.0963	35.5810
with	21	22	0.0904	0.3246	1.0900	35.4652
without	1	12	0.3836	0.2225	1.0688	35.0655
with	1	12	0.3276	0.2221	1.0116	33.9063
without	1	11	0.3836	0.2225	1.0688	35.0655
with	1	11	0.3276	0.2221	1.0116	33.9063
without	4	18	0.3836	0.2225	1.0688	35.0655
with	4	18	0.3276	0.2221	1.0116	33.9063
without	4	19	0.3836	0.2225	1.0688	35.0655
with	4	19	0.3276	0.2221	1.0116	33.9063
without	7	8	0.1561	0.2910	1.0524	34.7451
with	7	8	0.1410	0.2905	1.0358	34.4114
without	22	23	0.1561	0.2910	1.0524	34.7451
with	22	23	0.1410	0.2905	1.0358	34.4114
without	23	24	0.1561	0.2910	1.0524	34.7451
with	23	24	0.1410	0.2905	1.0358	34.4114
without	6	7	0.1561	0.2910	1.0524	34.7451
with	6	7	0.1410	0.2905	1.0358	34.4114
without	3	12	0.3771	0.2161	1.0428	34.5527
with	3	12	0.4343	0.2160	1.0997	35.6429
without	2	18	0.3771	0.2161	1.0428	34.5527
with	2	18	0.4343	0.2160	1.0997	35.6429
without	3	19	0.3771	0.2161	1.0428	34.5527
with	3	19	0.4343	0.2160	1.0997	35.6429
without	2	11	0.3771	0.2161	1.0428	34.5527
with	2	11	0.4343	0.2160	1.0997	35.6429
without	8	12	0.2966	0.2401	1.0361	34.4178
with	8	12	0.3044	0.2399	1.0434	34.5643

Table 49: Continue of Table 48

The procedure	i	j	$ \theta_i - \theta_j $	σ_{ij}	$\frac{ \theta_i - \theta_j + 3.08 \sigma_{ij}}{3.08 \sigma_{ij}}$	$\frac{l_{ij} \sin(\theta_i - \theta_j + 3.08 \sigma_{ij})}{+3.08 \sigma_{ij}}$
without	18	22	0.2966	0.2401	1.0361	34.4178
with	18	22	0.3044	0.2399	1.0434	34.5643
without	19	24	0.2966	0.2401	1.0361	34.4178
with	19	24	0.3044	0.2399	1.0434	34.5643
without	6	11	0.2966	0.2401	1.0361	34.4178
with	6	11	0.3044	0.2399	1.0434	34.5643
without	17	18	0.2529	0.2468	1.0132	33.9414
with	17	18	0.2452	0.2468	1.0055	33.7763
without	12	13	0.2529	0.2468	1.0132	33.9414
with	12	13	0.2452	0.2468	1.0055	33.7763
without	10	11	0.2529	0.2468	1.0132	33.9414
with	10	11	0.2452	0.2468	1.0055	33.7763
without	19	20	0.2529	0.2468	1.0132	33.9414
with	19	20	0.2452	0.2468	1.0055	33.7763
without	5	10	0.1402	0.2697	0.9709	33.0156
with	5	10	0.1478	0.2699	0.9792	33.2026
without	9	13	0.1402	0.2697	0.9709	33.0156
with	9	13	0.1478	0.2699	0.9792	33.2026
without	20	25	0.1402	0.2697	0.9709	33.0156
with	20	25	0.1478	0.2699	0.9792	33.2026
without	17	21	0.1402	0.2697	0.9709	33.0156
with	17	21	0.1478	0.2699	0.9792	33.2026
without	14	17	0.0896	0.2618	0.8960	31.2337
with	14	17	0.1047	0.2622	0.9123	31.6369
without	13	16	0.0896	0.2618	0.8960	31.2337
with	13	16	0.1047	0.2622	0.9123	31.6369
without	10	14	0.0896	0.2618	0.8960	31.2337
with	10	14	0.1047	0.2622	0.9123	31.6369
without	16	20	0.0896	0.2618	0.8960	31.2337
with	16	20	0.1047	0.2622	0.9123	31.6369
without	1	15	0.0530	0.1622	0.5526	20.9973
with	1	15	5.0008e-04	0.1625	0.5010	19.2139
without	4	15	0.0530	0.1622	0.5526	20.9973
with	4	15	4.9992e-04	0.1625	0.5010	19.2139
without	3	15	0.0470	0.1506	0.5110	19.5606
with	3	15	0.0997	0.1506	0.5635	21.3651
without	2	15	0.0470	0.1506	0.5110	19.5606
with	2	15	0.0997	0.1506	0.5635	21.3651

Table 50: Tail Probability of the Manhattan network according to Table 48

The procedure	i	j	$P(\omega \in \Omega \mid \theta_{ij}(\omega, t) < -\pi/2)$	$P(\omega \in \Omega \mid \theta_{ij}(\omega, t) > \pi/2)$	by our criterion (Upper bound)
without	1	7	1.4337e-12	3.0303e-04	
with	1	7	2.3681e-12	1.8144e-04	$2 \times 1.8171e - 04$
without	4	23	1.4337e-12	3.0303e-04	
with	4	23	2.3681e-12	1.8144e-04	$2 \times 1.8171e - 04$
without	2	14	4.8713e-19	1.2856e-05	
with	2	14	1.7850e-19	2.6386e-05	$2 \times 1.1583e - 04$
without	3	16	4.8713e-19	1.2856e-05	
with	3	16	1.7850e-19	2.6386e-05	$2 \times 1.1583e - 04$
without	5	6	2.7707e-06	1.3226e-07	
with	5	6	2.5494e-06	1.5466e-07	$2 \times 2.0917e - 04$
without	24	25	1.3226e-07	2.7707e-06	
with	24	25	1.5466e-07	2.5494e-06	$2 \times 2.0917e - 04$
without	8	9	1.3226e-07	2.7707e-06	
with	8	9	1.5466e-07	2.5494e-06	$2 \times 2.0917e - 04$
without	21	22	2.7707e-06	1.3226e-07	
with	21	22	2.5494e-06	1.5466e-07	$2 \times 2.0917e - 04$
without	1	12	7.9019e-19	4.7585e-08	
with	1	12	6.2900e-18	1.0876e-08	$2 \times 9.3823e - 05$
without	1	11	7.9019e-19	4.7585e-08	
with	1	11	6.2900e-18	1.0876e-08	$2 \times 9.3823e - 05$
without	4	18	7.9019e-19	4.7585e-08	
with	4	18	6.2900e-18	1.0876e-08	$2 \times 9.3823e - 05$
without	4	19	7.9019e-19	4.7585e-08	
with	4	19	6.2900e-18	1.0876e-08	$2 \times 9.3823e - 05$
without	7	8	1.4750e-09	5.8250e-07	
with	7	8	1.9010e-09	4.2866e-07	$2 \times 1.7124e - 04$
without	22	23	5.8250e-07	1.4750e-09	
with	22	23	4.2866e-07	1.9010e-09	$2 \times 1.7124e - 04$
without	23	24	1.4750e-09	5.8250e-07	
with	23	24	1.9010e-09	4.2866e-07	$2 \times 1.7124e - 04$
without	6	7	5.8250e-07	1.4750e-09	
with	6	7	4.2866e-07	1.9010e-09	$2 \times 1.7124e - 04$
without	3	12	9.9459e-20	1.6586e-08	
with	3	12	8.2500e-21	7.1420e-08	$2 \times 8.7159e - 05$
without	2	18	9.9459e-20	1.6586e-08	
with	2	18	8.2500e-21	7.1420e-08	$2 \times 8.7159e - 05$
without	3	19	9.9459e-20	1.6586e-08	
with	3	19	8.2500e-21	7.1420e-08	$2 \times 8.7159e - 05$
without	2	11	9.9459e-20	1.6586e-08	
with	2	11	8.2500e-21	7.1420e-08	$2 \times 8.7159e - 05$

Table 51: Tail Probability of the Manhattan network according to Table 49

The procedure	i	j	$P(\omega \in \Omega \mid \theta_{ij}(\omega, t) < -\pi/2)$	$P(\omega \in \Omega \mid \theta_{ij}(\omega, t) > \pi/2)$	by our criterion (Upper bound)
without	8	12	5.5740e-08	3.6963e-15	
with	8	12	6.4998e-08	2.7140e-15	$2 \times 1.1369e - 04$
without	18	22	3.6963e-15	5.5740e-08	
with	18	22	2.7140e-15	6.4998e-08	$2 \times 1.1369e - 04$
without	19	24	3.6963e-15	5.5740e-08	
with	19	24	2.7140e-15	6.4998e-08	$2 \times 1.1369e - 04$
without	6	11	5.5740e-08	3.6963e-15	
with	6	11	6.4998e-08	2.7140e-15	$2 \times 1.1369e - 04$
without	17	18	4.6490e-08	7.3763e-14	
with	17	18	3.9121e-08	9.3224e-14	$2 \times 1.2150e - 04$
without	12	13	7.3763e-14	4.6490e-08	
with	12	13	9.3224e-14	3.9121e-08	$2 \times 1.2150e - 04$
without	10	11	4.6490e-08	7.3763e-14	
with	10	11	3.9121e-08	9.3224e-14	$2 \times 1.2150e - 04$
without	19	20	7.3763e-14	4.6490e-08	
with	19	20	9.3224e-14	3.9121e-08	$2 \times 1.2150e - 04$
without	5	10	5.6523e-08	1.1188e-10	
with	5	10	6.7359e-08	9.6048e-11	$2 \times 1.4783e - 04$
without	9	13	5.6523e-08	1.1188e-10	
with	9	13	6.7359e-08	9.6048e-11	$2 \times 1.4783e - 04$
without	20	25	1.1188e-10	5.6523e-08	
with	20	25	9.6048e-11	6.7359e-08	$2 \times 1.4783e - 04$
without	17	21	1.1188e-10	5.6523e-08	
with	17	21	9.6048e-11	6.7359e-08	$2 \times 1.4783e - 04$
without	14	17	1.1323e-10	7.6690e-09	
with	14	17	8.2864e-11	1.1255e-08	$2 \times 1.3904e - 04$
without	13	16	7.6690e-09	1.1323e-10	
with	13	16	1.1255e-08	8.2864e-11	$2 \times 1.3904e - 04$
without	10	14	7.6690e-09	1.1323e-10	
with	10	14	1.1255e-08	8.2864e-11	$2 \times 1.3904e - 04$
without	16	20	1.1323e-10	7.6690e-09	
with	16	20	8.2864e-11	1.1255e-08	$2 \times 1.3904e - 04$
without	1	15	6.8132e-24	4.0799e-21	
with	1	15	2.0315e-22	2.1573e-22	$2 \times 3.5136e - 05$
without	4	15	6.8132e-24	4.0799e-21	
with	4	15	2.0315e-22	2.1573e-22	$2 \times 3.5136e - 05$
without	3	15	3.2196e-27	2.2946e-24	
with	3	15	6.8384e-29	7.7056e-23	$2 \times 2.6038e - 05$
without	2	15	3.2196e-27	2.2946e-24	
with	2	15	6.8384e-29	7.7056e-23	$2 \times 2.6038e - 05$

Table 52: Phase-angle differences and other outputs for Manhattan network without and with control, power demand vector symmetric, disturbance vector asymmetric

The procedure	i	j	$ \theta_i - \theta_j $	σ_{ij}	$\frac{ \theta_i - \theta_j + 3.08 \sigma_{ij}}{3.08 \sigma_{ij}}$	$\frac{l_{ij} \sin(\theta_i - \theta_j + 3.08 \sigma_{ij})}{3.08 \sigma_{ij}}$
without	1	7	0.5363	0.3149	1.5062	39.9165
with	1	7	0.4990	0.3128	1.4625	39.7656
without	4	23	0.5363	0.3128	1.4997	39.8990
with	4	23	0.5046	0.3110	1.4625	39.7656
without	3	16	0.5574	0.2589	1.3550	39.0719
with	3	16	0.5932	0.2601	1.3943	39.3787
without	2	14	0.5574	0.2590	1.3550	39.0725
with	2	14	0.5932	0.2600	1.3941	39.3770
without	5	6	0.0979	0.3412	1.1489	36.4920
with	5	6	0.0896	0.3416	1.1416	36.3717
without	8	9	0.0979	0.3377	1.1380	36.3114
with	8	9	0.0896	0.3381	1.1310	36.1934
without	24	25	0.0979	0.3304	1.1154	35.9243
with	24	25	0.0912	0.3307	1.1099	35.8256
without	6	7	0.1561	0.3109	1.1138	35.8953
with	6	7	0.1397	0.3104	1.0959	35.5731
without	19	24	0.2966	0.2631	1.1068	35.7715
with	19	24	0.3040	0.2628	1.1135	35.8899
without	21	22	0.0979	0.3275	1.1065	35.7661
with	21	22	0.0912	0.3279	1.1012	35.6696
without	23	24	0.1561	0.3071	1.1019	35.6832
with	23	24	0.1422	0.3068	1.0870	35.4102
without	7	8	0.1561	0.3068	1.1010	35.6670
with	7	8	0.1397	0.3062	1.0829	35.3328
without	6	11	0.2966	0.2599	1.0971	35.5958
with	6	11	0.3049	0.2597	1.1046	35.7320
without	1	12	0.3836	0.2299	1.0916	35.4955
with	1	12	0.3233	0.2295	1.0302	34.2956
without	1	11	0.3836	0.2285	1.0874	35.4173
with	1	11	0.3233	0.2281	1.0259	34.2074
without	22	23	0.1561	0.3016	1.0849	35.3708
with	22	23	0.1422	0.3011	1.0695	35.0788
without	8	12	0.2966	0.2549	1.0816	35.3077
with	8	12	0.3049	0.2547	1.0895	35.4555
without	10	11	0.2529	0.2681	1.0787	35.2529
with	10	11	0.2439	0.2681	1.0695	35.0792
without	4	19	0.3836	0.2253	1.0776	35.2324
with	4	19	0.3319	0.2250	1.0250	34.1878
without	19	20	0.2529	0.2672	1.0759	35.2016
with	19	20	0.2465	0.2672	1.0694	35.0757

Table 53: Continue of Table 52

The procedure	i	j	$ \theta_i - \theta_j $	σ_{ij}	$\frac{ \theta_i - \theta_j + 3.08 \sigma_{ij}}{3.08 \sigma_{ij}}$	$\frac{l_{ij} \sin(\theta_i - \theta_j + 3.08 \sigma_{ij})}{3.08 \sigma_{ij}}$
without	3	12	0.3771	0.2233	1.0650	34.9921
with	3	12	0.4379	0.2233	1.1255	36.0993
without	2	11	0.3771	0.2218	1.0602	34.8979
with	2	11	0.4379	0.2214	1.1199	36.0019
without	12	13	0.2529	0.2614	1.0582	34.8588
with	12	13	0.2439	0.2615	1.0495	34.6861
without	4	18	0.3836	0.2184	1.0562	34.8204
with	4	18	0.3319	0.2180	1.0033	33.7302
without	3	19	0.3771	0.2182	1.0493	34.6824
with	3	19	0.4307	0.2180	1.1022	35.6882
without	18	22	0.2966	0.2415	1.0404	34.5038
with	18	22	0.3040	0.2414	1.0475	34.6473
without	2	18	0.3771	0.2113	1.0278	34.2468
with	2	18	0.4307	0.2112	1.0812	35.3018
without	20	25	0.1402	0.2863	1.0220	34.1257
with	20	25	0.1470	0.2866	1.0297	34.2848
without	17	18	0.2529	0.2494	1.0211	34.1071
with	17	18	0.2465	0.2495	1.0149	33.9772
without	9	13	0.1402	0.2836	1.0137	33.9513
with	9	13	0.1486	0.2837	1.0224	34.1340
without	5	10	0.1402	0.2800	1.0026	33.7152
with	5	10	0.1486	0.2803	1.0119	33.9140
without	16	20	0.0896	0.2848	0.9667	32.9210
with	16	20	0.1026	0.2852	0.9809	33.2407
without	10	14	0.0896	0.2810	0.9552	32.6562
with	10	14	0.1068	0.2813	0.9731	33.0644
without	17	21	0.1402	0.2644	0.9547	32.6449
with	17	21	0.1470	0.2647	0.9621	32.8154
without	13	16	0.0896	0.2795	0.9506	32.5503
with	13	16	0.1068	0.2799	0.9689	32.9717
without	14	17	0.0896	0.2713	0.9252	31.9498
with	14	17	0.1026	0.2717	0.9396	32.2931
without	4	15	0.0530	0.1928	0.6468	24.1064
with	4	15	0.0079	0.1931	0.6025	22.6696
without	1	15	0.0530	0.1928	0.6468	24.1067
with	1	15	0.0069	0.1932	0.6018	22.6465
without	2	15	0.0470	0.1859	0.6197	23.2325
with	2	15	0.0997	0.1859	0.6723	24.9118
without	3	15	0.0470	0.1854	0.6181	23.1804
with	3	15	0.0997	0.1854	0.6706	24.8577

Table 54: Tail Probability of the Manhattan network according to Table 52

The procedure	i	j	$P(\omega \in \Omega \mid \theta_{ij}(\omega, t) < -\pi/2)$	$P(\omega \in \Omega \mid \theta_{ij}(\omega, t) > \pi/2)$	by our criterion (Upper bound)
without	1	7	1.1058e-11	5.0963e-04	
with	1	7	1.8329e-11	3.0575e-04	$2 \times 3.0603e - 04$
without	4	23	8.1268e-12	4.7115e-04	
with	4	23	1.2506e-11	3.0370e-04	$2 \times 3.0378e - 04$
without	3	16	1.0163e-16	4.5345e-05	
with	3	16	4.4033e-17	8.5454e-05	$2 \times 2.3582e - 04$
without	2	14	1.0435e-16	4.5630e-05	
with	2	14	4.2860e-17	8.4961e-05	$2 \times 2.3568e - 04$
without	5	6	7.9149e-06	5.0247e-07	
with	5	6	7.2531e-06	5.8502e-07	$2 \times 3.4061e - 04$
without	8	9	3.8790e-07	6.4571e-06	
with	8	9	4.5315e-07	5.9084e-06	$2 \times 3.3655e - 04$
without	24	25	2.2029e-07	4.1380e-06	
with	24	25	2.5081e-07	3.8361e-06	$2 \times 3.2783e - 04$
without	6	7	2.6781e-06	1.3920e-08	
with	6	7	2.0086e-06	1.7879e-08	$2 \times 3.0302e - 04$
without	19	24	6.3440e-13	6.3943e-07	
with	19	24	4.8772e-13	7.1642e-07	$2 \times 2.3963e - 04$
without	21	22	3.4396e-06	1.7414e-07	
with	21	22	3.2058e-06	2.0037e-07	$2 \times 3.2449e - 04$
without	23	24	9.3706e-09	2.0462e-06	
with	23	24	1.1791e-08	1.6086e-06	$2 \times 2.9849e - 04$
without	7	8	9.0767e-09	2.0024e-06	
with	7	8	1.1604e-08	1.4789e-06	$2 \times 2.9773e - 04$
without	6	11	4.7278e-07	3.3590e-13	
with	6	11	5.4554e-07	2.5511e-13	$2 \times 2.3526e - 04$
without	1	12	9.3924e-18	1.2088e-07	
with	1	12	7.7141e-17	2.7289e-08	$2 \times 1.9125e - 04$
without	1	11	5.9884e-18	1.0203e-07	
with	1	11	5.0418e-17	2.2619e-08	$2 \times 1.8915e - 04$
without	22	23	1.3618e-06	5.1479e-09	
with	22	23	1.0446e-06	6.3845e-09	$2 \times 2.9121e - 04$
without	8	12	2.8843e-07	1.1857e-13	
with	8	12	3.3451e-07	8.9016e-14	$2 \times 2.2814e - 04$
without	10	11	4.4235e-07	5.1481e-12	
with	10	11	3.7248e-07	6.4959e-12	$2 \times 2.4705e - 04$
without	4	19	2.0743e-18	6.8434e-08	
with	4	19	1.3785e-17	1.8332e-08	$2 \times 1.8450e - 04$
without	19	20	4.3898e-12	4.0645e-07	
with	19	20	5.1854e-12	3.5943e-07	$2 \times 2.4579e - 04$

Table 55: Tail Probability of the Manhattan network according to Table 53

The procedure	i	j	$P(\omega \in \Omega \mid \theta_{ij}(\omega, t) < -\pi/2)$	$P(\omega \in \Omega \mid \theta_{ij}(\omega, t) > \pi/2)$	by our criterion (Upper bound)
without	3	12	1.3519e-18	4.5032e-08	
with	3	12	1.1757e-19	1.9536e-07	$2 \times 1.8194e - 04$
without	2	11	8.0140e-19	3.6860e-08	
with	2	11	5.8050e-20	1.5524e-07	$2 \times 1.7908e - 04$
without	12	13	1.5115e-12	2.3073e-07	
with	12	13	1.9665e-12	1.9459e-07	$2 \times 2.3780e - 04$
without	4	18	1.7984e-19	2.7263e-08	
with	4	18	1.2965e-18	6.6172e-09	$2 \times 1.7393e - 04$
without	3	19	2.1863e-19	2.2419e-08	
with	3	19	2.1320e-20	8.4847e-08	$2 \times 1.7393e - 04$
without	18	22	5.2732e-15	6.5954e-08	
with	18	22	4.0391e-15	7.7002e-08	$2 \times 2.0887e - 04$
without	2	18	1.5046e-20	8.0553e-09	
with	2	18	1.3112e-21	3.3660e-08	$2 \times 1.6359e - 04$
without	20	25	1.1418e-09	2.9138e-07	
with	20	25	1.0256e-09	3.3843e-07	$2 \times 2.7224e - 04$
without	17	18	6.3104e-08	1.3127e-13	
with	17	18	5.5478e-08	1.6233e-13	$2 \times 2.2066e - 04$
without	9	13	2.2745e-07	8.0406e-10	
with	9	13	2.6790e-07	6.7801e-10	$2 \times 2.6836e - 04$
without	5	10	1.6170e-07	4.9597e-10	
with	5	10	1.9494e-07	4.2814e-10	$2 \times 2.6378e - 04$
without	16	20	2.7707e-09	9.9200e-08	
with	16	20	2.2128e-09	1.3167e-07	$2 \times 2.7037e - 04$
without	10	14	6.7782e-08	1.7222e-09	
with	10	14	9.7315e-08	1.2327e-09	$2 \times 2.6513e - 04$
without	17	21	4.8600e-11	3.1385e-08	
with	17	21	4.3033e-11	3.7470e-08	$2 \times 2.4230e - 04$
without	13	16	5.8076e-08	1.4199e-09	
with	13	16	8.4560e-08	1.0265e-09	$2 \times 2.6324e - 04$
without	14	17	4.6744e-10	2.3857e-08	
with	14	17	3.6606e-10	3.2633e-08	$2 \times 2.5203e - 04$
without	4	15	1.8477e-17	1.7397e-15	
with	4	15	1.4727e-16	2.8936e-16	$2 \times 1.3588e - 04$
without	1	15	1.8477e-17	1.7397e-15	
with	1	15	1.5922e-16	2.8702e-16	$2 \times 1.3603e - 04$
without	2	15	1.6231e-18	1.2337e-16	
with	2	15	1.2820e-19	1.2525e-15	$2 \times 1.2486e - 04$
without	3	15	1.3194e-18	1.0263e-16	
with	3	15	1.0281e-19	1.0549e-15	$2 \times 1.2409e - 04$